UNIVERSIDADE D
COIMBRA

Gonçalo Filipe Almeida Santos

A STUDY OF CORTICAL MECHANISMS FOR SOLVING AMBIGUITY USING NON-INVASIVE HUMAN ELECTROPHYSIOLOGY

Dissertação no âmbito do Mestrado em Engenharia Biomédica orientada pelo Doutor Gabriel Nascimento Ferreira da Costa e pela Doutora Maria José Braga Marques Ribeiro apresentada à Faculdade de Ciências e Tecnologia da Universidade de Coimbra.

Fevereiro de 2023

Gonçalo Filipe Almeida Santos

A STUDY OF CORTICAL MECHANISMS FOR SOLVING AMBIGUITY USING NON-INVASIVE HUMAN ELECTROPHYSIOLOGY

Thesis submitted to the Faculty of Science and Technology of the University of Coimbra for the degree of Master in Biomedical Engineering with specialization in Biomedical Instrumentation

Supervisors:
Dr. Gabriel Nascimento Ferreira da Costa
Drª. Maria José Braga Marques Ribeiro

Coimbra, 2023

This work was developed in collaboration with:

ICNAS – Institute of Nuclear Sciences Applied to Health

Agradecimentos

Primeiramente, gostaria de agradecer fortemente ao meu orientador Gabriel Costa. Obrigado por ter estado sempre disponível para me ajudar e auxiliar em todos os assuntos que este trabalho exigiu, por toda a prontidão e apoio que me disponibilizou, por acreditar em mim e neste projeto a 100 %. É uma pessoa incrível de se trabalhar e conviver e por isso só tenho de agradecer a sorte que tive de o escolher como orientador. Uma palavra de agradecimento também direcionada à Maria Ribeiro por também prestar sempre um apoio e uma presença fundamental sempre que preciso para a elaboração correta deste trabalho. O meu sincero obrigado a estas duas pessoas.

Quero agradecer também aos meus pais, eles que são a minha base e sustento da vida, por permitirem a oportunidade incrível e única de estudar em Coimbra e fazer aquilo que gosto. Obrigado por todo o apoio, amor, carinho e momentos incríveis. Sou um miúdo privilegiado por vos ter como pais. Agradecer também em especial ao meu irmão e à minha irmã, às minhas avós, os meus tios e prima, por darem me uma estrutura familiar maravilhosa e amo-vos muito a todos.

Deixar um agradecimento em especial também à minha Marianinha, por me ter acompanhado de perto toda esta jornada da minha vida e que espero que continue ao meu lado na minha vida por muito tempo. Obrigado por estares sempre presente e me apoiares em todas as maluquices que nos lembramos, somos felizes assim ao menos.

Por fim, agradecer aos meus amigos por proporcionarem momentos e memórias lindas tanto nos últimos 5 anos em Coimbra, as noites e convívios passados com os BCL ou com o meu colega Pedro, e também agradecer em especial aos meus amigos mais lindos de Faro, Ruivo e Nader, e os meus amigos de longa data, Miguel e António. Obrigado por tudo.

Resumo

Quando um estímulo permanece inalterado, mas que pode ter diferentes interpretações, ele é considerado ambíguo. O sistema visual é constantemente estimulado por estímulos ambíguos e quando observado por longos períodos de tempo, dá origem a uma competição entre as possíveis perceções do estímulo. Quando existem apenas duas interpretações possíveis, esses modos concorrentes de perceção alternam entre si, resultando num fenómeno denominado perceção biestável. As razões para esta mudança percetiva contínua, apenas parcialmente sobre o nosso controlo cognitivo e em grande parte sujeita a mecanismos estocásticos, levantam questões cruciais: quais os mecanismos cerebrais que são responsáveis pela competição e pela "quase" estabilidade dessas configurações competitivas?

O trabalho descrito em Costa et al. (2017) apresenta um estímulo ambíguo que consistia num padrão listado simétrico, com linhas pretas anguladas sobre um fundo branco, formando uma figura semelhante a um padrão de "telhado". Para este estímulo, foi possível interpretá-lo de duas formas: "Bound", com movimento descendente e "Unbound", com movimento para dentro em direção ao eixo central do estímulo.

Usando os mesmos conjuntos de dados de EEG adquiridos no trabalho de Costa et al. (2017), o objetivo principal foi explorar a relação entre os potenciais relacionados a eventos (ERPs) dos períodos de mudança percetiva com a atividade oscilatória do EEG, mais especificamente as ondas beta (13-30 Hz). Primeiro, os ERPs no momento da mudança percetiva foram estudados considerando eventos distintos de mudança percetual: as transições podem resultar da mudança da perceção de Bound para Unbound (BU) ou de uma configuração Unbound para Bound (UB). Esses ERPs de troca perceptual exibem características que separam os dois eventos percetivos e mostram uma dinâmica semelhante à modulação da atividade beta em torno do momento da mudança percetiva. Os nossos resultados mostraram ainda que um método apropriado para estudar esses eventos é usar o método reference-free Surface

Laplacian/CSD, pois tem uma maior resolução espacial e maior especificidade, evitando enviesar sinais para regiões não relacionadas com o estudo. Durante as mudanças percetivas, descobriu-se que os ERPs proeminentes nas regiões parietal e occipital exibiam dinâmicas distintas quando a perceção mudava de uma perceção para outra. As componentes do ERP identificados também mostraram uma dinâmica lenta, sugerindo que estes poderiam resultar de potenciais que se estendem além da janela de mudança percetiva. Numa segunda parte do trabalho, foram analisados períodos em que as perceções permaneceram estáveis para entender a variação dos potenciais muitos segundos após a ocorrência da mudança percetiva. Isso revelou que esses potenciais são de fato duradouros e podem ser medidos mesmo durante períodos estáveis de perceção. Por fim, propusemos testar uma hipótese para a relação entre ERPs e as oscilações cerebrais: as componentes lentas dos potenciais são consequência da modulação assimétrica da amplitude da atividade oscilatória no cérebro. Utilizámos o modelo proposto por Mazaheri e Jensen (2008) para calcular o índice de assimetria AFA_{index} nos dados simulados e nos dados empíricos em estudo, e assim entender se a assimetria poderia ser a causa das modulações observadas nos ERPs. Mostrámos que o índice AFA_{index} é uma boa medida para averiguar a assimetria das oscilações, mas que os valores registados nos dados empíricos não mostram diferenças entre condições de mudança percetiva e condições de referência de perceção estável, portanto, este modelo provavelmente não explica as componentes lentas dos ERPs. No entanto, a questão sobre a relação existente entre as oscilações beta e as modulações lentas observadas nos ERPs deste estudo permanece em aberto.

Palavras-chave: EEG, ERP, Oscilações cerebrais, Perceção Biestável, Assimetria, Referência, Movimento

Abstract

When a stimulus remains unchanged, but can have different interpretations, it is considered ambiguous. The visual system is constantly stimulated by ambiguous stimuli which when observed for long periods of time give rise to a competition between possible perceptions. When only two possible interpretations exist these competing modes of perceiving alternate with one another resulting in a phenomenon called bistable perception. This continuous perceptual switch, only partially under our cognitive control and largely subject to stochastic mechanisms, raises crucial questions: what are the brain mechanisms responsible for the competition and quase-stability of these competing configurations?

The work described in Costa et al. (2017) investigates the mechanisms underlying the perception of an ambiguous stimulus that consisted of a symmetrical striped pattern, with angled black lines on a white background, forming a figure similar to a "roof" pattern. For this stimulus, it was possible to interpret it in two ways: "Bound", with a downward movement and "Unbound", with an inward movement towards the central axis of the stimulus.

Using the same EEG dataset acquired by Costa et al. (2017), the main objective of the current work was to explore the relationship between the event-related potentials (ERPs) evoked by perceptual switches and the oscillatory activity of the EEG, more specifically the beta waves (13-30 Hz). First, ERPs at the moment of perceptual change were studied considering distinct perceptual switch events: transitions could result from perception changing from Bound to Unbound (BU) or from an Unbound to a Bound configuration (UB). These perceptual-switch ERPs display characteristics that set the two perceptual events apart and show a similar dynamics as the modulation of beta activity around the moment of perceptual change. Our results further showed that an appropriate method of studying these events is to use the Surface Laplacian/CSD reference-free method, as it has a higher spatial resolution and greater specificity avoiding biassing signals to unrelated areas. During perceptual switches it

was found that ERPs prominent in parietal and occipital regions displayed distinct dynamics when perception switched from one to another percept. The ERP components identified also showed a slow dynamic, suggesting that these could result from potentials which extend beyond the window of perceptual switch. In a second part of the work, periods in which perceptions remained stable were analysed to understand the variation of potentials many seconds after the perceptual change happened. This revealed that these potentials are in fact long-lasting and can be measured even during stable periods of perception. Lastly, we proposed to test a hypothesis for the relationship between ERPs and brain oscillations: slow components of potentials are a consequence of asymmetric modulation of the amplitude of oscillatory activity in the brain. We used the model proposed by Mazaheri and Jensen (2008) to calculate the asymmetry index AFA_{index} in simulated data and in the empirical data under study, and thus understand whether asymmetry could be the cause of the modulations observed in ERPs. We showed that the AFA_{index} is a good measure to ascertain the asymmetry of the oscillations, but that the one registered in the empirical does not show differences between conditions of perceptual change and reference conditions of stable perception, hence, this model likely does not explain the slow components of the ERPs. However, the question about the relationship that exists between the beta oscillations and the slow modulations observed in the ERPs of this study remains open.

Keywords: EEG, ERP, Brain Oscillations, Bistable Perception, Asymmetry, Reference, Motion

Table of Contents

List of Figures

List of Abbreviations

AFA – Amplitude Fluctuation Asymmetry. 32, 33, 34, 55, 56, 57, 58, 59.

BCI – Brain Computer Interfaces. 12.

BU – Bound-to-Unbound. 29, 31, 32, 34, 35, 38, 39, 40, 44, 45, 46, 48, 50, 51, 52, 53, 57, 58, 59.

CSD – Current Source Density. 27, 30, 34, 38, 46, 47, 49, 50, 57, 58, 60, 61, 62, 65.

EEG – Electroencephalography. 12, 13, 14, 15, 16, 17, 19, 20, 21, 22, 25, 26, 27, 28, 29, 30, 32, 33, 34, 36, 38, 40, 41, 46, 48, 51, 54, 55, 57, 59, 62, 64, 65.

ERP – Event-Related Potential. 16, 17, 19, 20, 21, 22, 23, 24, 28, 30, 31, 34, 35, 36, 38, 39, 40, 41, 42, 43, 44, 46, 47, 48, 49, 53, 54, 57, 62, 63, 64, 65.

fMRI – Functional Magnetic Resonance Imaging. 63.

hMT – Human Medial Temporal Area. 63, 64.

ICA – Independent Components Analysis. 27, 28.

IPS – Intraparietal Sulcus. 9.

IT – Inferior Temporal Cortex. 3.

LFP – Local Field Potential. 13.

LGN – Lateral Geniculate Nucleus. 3, 8, 9.

MEG – Magnetoencephalography. 21, 63, 65.

MST – Medial Superior Temporal Area. 5, 8, 11.

MT/V5 – Medial Temporal Area. 2, 3, 5, 8, 9, 11, 63.

PPC – Posterior Parietal Cortex. 3.

SB – Stable Perception Epochs of Bound Configuration. 29, 34, 35, 60, 61.

SCD – Scalp Current Density. 30.

SU – Stable Perception Epochs of Unbound Configuration. 29, 34, 35, 60, 61.

UB – Unbound-to-Bound. 29, 31, 32, 34, 35, 38, 39, 40, 41, 44, 45, 46, 48, 50, 51, 52, 53, 57, 58, 59.

V1 – Primary Visual Cortex. 2, 3, 4, 8, 9, 11.

1. Introduction

In this introductory chapter of the thesis, I will explain the motivation behind the current work which builds on previous findings relating to perceptual organisation in vision. Some of the main concepts of vision, cortical electrical potentials and rhythms addressed in the current work are described in the following sections. Finally, the objectives driving the current work are explained in detail.

1.1. Motivation

Many aspects of the science of vision and perception remain to be fully understood. The fact that vision relies on the brain interpreting an exterior three-dimensional world from light signals that are captured by a small two-dimensional layer of photosensitive cells in the retina already suggests that information can be lost and very likely has to be inferred. Thus, the brain deals with a constant level of ambiguity, that is, visual stimuli that while producing a single pattern of activity in the retina can still be interpreted in different ways. The question then arises of what is behind the brain decisions that lead to perceiving something in one way at one moment, and something different at another moment.

Much of the recorded brain activity is the sum of neuronal populations undergoing active at different levels and distinct modes which manifest in different oscillatory signals. Oscillations in the beta frequency band have been shown to play a role on perceptual decision mechanisms. Following previous findings of beta oscillations correlating with perception under ambiguity and rivalry, the work in Costa et al., (2017) demonstrates a large activity in the beta frequency band that characterize perceptual changes and perceptual interpretations when viewing ambiguous moving stimuli. The motivation for the current study is to build on those findings by looking at potentials that drive perception, rather than non-phase locked oscillations. The timing and magnitude of potentials during perceptual change events was found to have

similar dynamics as the beta oscillations which led us to further try to explain how both signals could be related and perhaps clarify the mechanisms for solving perceptual ambiguity.

1.2. Background

1.2.1. Visual Cortex

The visual cortex is the area of the brain responsible for processing, segmenting and also integrating the visual information we receive through our eyes, and which shapes our interpretation of the world around us. The visual cortex is the centre of our perception of movement, colour, shapes and depth. Damage to the more primary areas of the visual cortex can thus result in the total loss of vision of visual fields represented in the activity of those damaged neurons.

The visual cortex is mainly located in the occipital lobe, reaching areas of the parietal and temporal lobes. As with most sensory paths of the vertebrate brain, contralateral processing is present in the visual cortex. Hence, the part of the cortex that makes up the left hemisphere of the brain receives information regarding the right visual field, while the part of the right hemisphere processes information from the left visual field. It is divided into two main zones: the striate cortex or primary visual cortex (V1) and the extra striate cortex composed of areas V2 (secondary visual cortex), V3, V4 and V5 (MT). Visual information is processed in each designated area and passed on to the next for more complex analyses, that is, the next area in the process is always more specialized than the previous one. This type of process is highly specialized and made to recognize patterns and objects seemingly effortlessly. Although this segmentation and interpretation of visual information is very reliable it can sometimes be faced with ambiguities which can lead to different interpretations of the same visual information (Huff and Prasanna Tadi, 2019).

About 90% of visual information from the eyes reaches the primary visual cortex via the lateral geniculate nucleus (LGN). This area is located in the calcarine cortex and

is surrounded by region V2 and more externally by V3 (Wandell, Dumoulin and Brewer, 2007). As with most cortical structures in the mammalian brain, it is made up of 6 layers of cells and these can be simple or complex depending on the complexity of their responses to the stimulus. Mostly at this stage neurons display sensitivity to luminance-defined oriented stimuli, such as dark and bright bars and gratings oriented in multiple directions, and simple forms of motion. From V1, the information is passed to the following area: V2. There is then an increase in the complexity of visual processing and also feedback communication with the previous area. Here the cells detect contours and combinations of orientation, contributing to the identification of more complex shapes (Anzai, Peng and Van Essen, 2007). Then the information can be seen as broadly following two pathways. The dorsal stream is composed by visual areas that process the location of objects and are in the posterior/superior part of the brain. This stream starts at V1, passes through V2, crosses V3 and MT/V5 (medial temporal area) and reaches the posterior parietal cortex (PPC). The ventral stream consists mainly of areas related to the classification of visual content and objects and is located in the inferior part of the occipital and temporal brain. This stream shares the same origin as the dorsal stream, starting with processing in V1 and V2, but then follows a more ventral pathway through V4 and reaching the inferior temporal cortex (IT) which shows a higher level of specialization (Tong, 2003; Goodale, 2011)

Area V3 is also divided in a dorsal and ventral area and receives information from both V2 and directly from V1 through inputs that bypass V2. The responses of its cells are related to orientation, motion and depth. Most of the information that reaches the V4 area comes from V2, although it has some connections with V1 and V3. Cells in this region are colour sensitive but also play a role in complex spatial and orientation tuning. Finally, area V5, also referred to as MT, has connections with V2 and V1, and is important for the processing of motion (Mather, 2016).

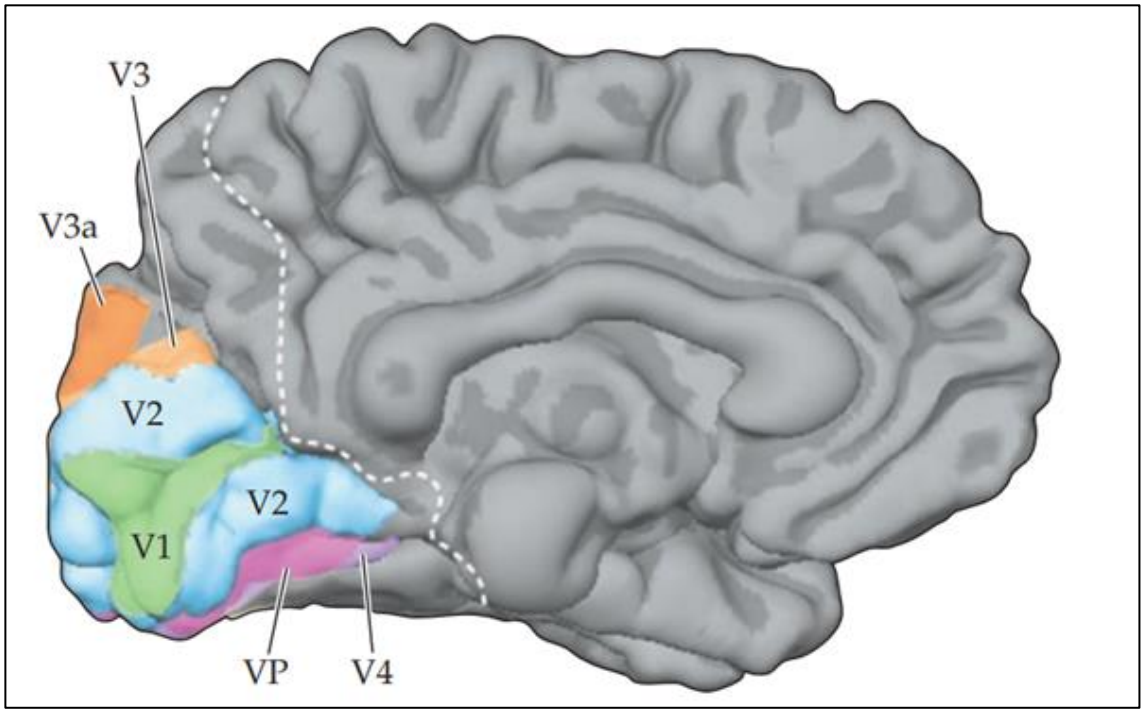

Figure 1.1. Localization of multiple visual areas in the human brain. Functional MRI yields medial view of the human brain, illustrating the location of primary visual cortex (V1) and additional visual areas V2 (blue), V3 (orange), VP (ventral posterior area, pink), V4 (purple). Reproduced from Purves (2018).

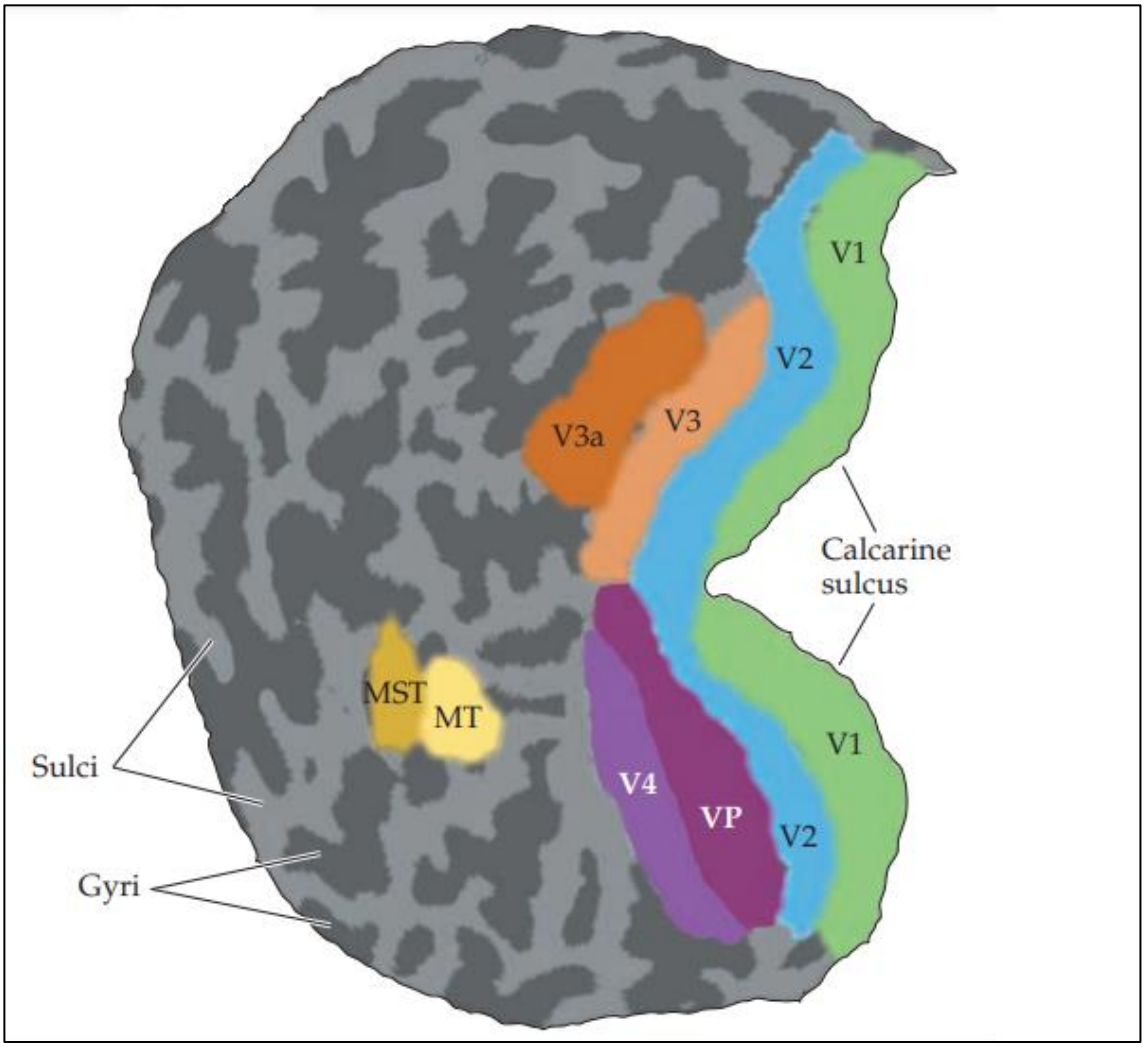

Figure 1.2. Representation of multiple visual areas with a flattened out occipital lobe in a human "inflated" brain. Unfolded and flattened view of retinotopically defined visual areas in the occipital lobe. Dark gray areas correspond to cortical regions buried in sulci; light regions correspond to regions that were located on the surface of gyri. Visual areas that were not possible to view in Figure 1.1 with a medial view are now exposed and visible in this representation, like MT and MST (medial superior temporal) area. Reproduced from Purves (2018).

1.2.2. Ambiguous Perception

A stimulus is an external or internal action or agent that causes a reaction to a system. Within the visual sensory context, stimuli are all the external actions that happen in the world that produce a brain response via the vision organs. The brain areas most involved in vision are the occipital ones which is where the information coming from the retina is perceived and decoded. Despite existing this direct correlation between stimulus and neuronal responses, in vision there are challenges to the correct interpretation of the visual world, including the ambiguity inherent to the visual information captured by the retinas.

Ambiguity is characterized by the lack of definitive information for the interpretation of the stimulus, that is, the stimulus can be interpreted in different ways depending on the observer's perspective or external factors and creates gaps in the interpretation of the exterior world. What can solve ambiguity could be something external such as nuances in stimulus or brain mechanisms that involve communication between different regions or interactions between bottom-up systems or top-down signals, the latter being more apt to provide information that has been learned and acquired through prolonged experience.

Inherently, all images that are created on the retina are ambiguous as observed by Gregory (1997), so several neural processes are needed that combine the images from both retinas and through this joint information, manage to overcome the obstacle of ambiguity and obtain a correct interpretation the incoming visual signals. However, sometimes a stimulus can be so ambiguous that the simple combination of retinal images is not enough to understand it.

In nature, that state of doubt does not usually happens, as the most common scenario is that our perspective being equivocally directly linked with reality, either from living in stable and safe situations or that our perceptual interpretation is adequate for the current stimulus and context. But it is also true that sometimes, certain stimuli evoke doubt, raising uncertainty between the surrounding physical world and our interpretation of it. One example of that disconnect are the different interpretations

of a physical object, when there is lack of crucial information of that same object presented outside of the visual field of the retina. In this hypothetical scenario, ambiguous plurality is generated, which in turn generates doubt in the observer (Brascamp and Shevell, 2021).

We also know that the world around us is made up of 3 dimensions, yet our perception is built from the combination of two 2D retinal images, which allows us to perceive depth in the visual world. In other words, as already mentioned, each retinal image is ambiguous because it can present different interpretations for the same physical object. But this is not the only source of ambiguity. Brascamp and Shevell (2021) highlight 3 factors capable of generating ambiguous perceptions: reverse optics, light and binocular rivalry.

The problem with inverse optics resides in that the brain infer the three-dimensional information of objects from a 2D image, i.e., after a reduction of information, specifically depth. In this way, there is an inherent ambiguity in vision, even if the combination with a second 2D image from the other eye provides depth information.

The aspect of light relates to how the illumination of physical objects plays a fundamental role in our perception. Light, reflection and shadows, all are factors that influence the interpretations of a single object, resulting in multiple solutions to interpreting the visual signals our brain receives. More specifically, the colour of an object, as well as its brightness and reflectance, are inferred from the light that bounces from that object but the amount and properties of light that bounces depends on the amount and quality of the light that illuminates that same object. This ambiguity in the true conditions of illumination of an object originates many illusions such as the recent blue-black vs white-golden dress (Rabin et al., 2016).

Lastly, a source of ambiguity that has been often the focus of vision research has to do with situations where the retinal images of each eye are completely different, either because there is an occluder or because the stimulus presents different aspects for each field of vision of each eye. This causes a condition known as binocular rivalry where, in most cases, the brain ignores the image of one eye and sees only what is shown to

the other eye. This condition manifests as a bistable state where from time to time the brain switches perception to the other eye.

1.2.3. Ambiguity on Visual Motion

A further aspect of vision that provides crucial information about our environment and how to interact with it is motion. Several features and cues from the visual input provide information regarding motion, which can represent a true continuous displacement of an object in the real world, or an illusion of motion implied from the quick succession of temporally correlated frames, i.e., as in the movies. In visual motion there are clear ambiguous aspects such as having to distinguish motion in the world and of its parts from the motion of the observer, which can also produce displacement of the visual world in the retina. Making sense of visual information in the presence of eye and body movement is a topic of continuous study and is known to require integration of proprioceptive signals and copies of efferent signals to muscles controlling ocular movements (Cavanaugh et al., 2016).

When the visual system detects retinal motion, this information has to be processed and integrated in order to be understood and decoded. The retina first sends this information to the LGN, which projects information mostly to the primary visual cortex (V1) but maintains some projections to the MT/V5 area. The cells in V1 are direction-selective and process motion as a 1-dimensional feature with local signals, that is, they are only sensitive to the direction of movement in a small region of the visual field (Teichmann, Edwards and Baker, 2021). In the MT/V5 region, different V1 projections that have local signals are integrated together to obtain a global perception and coherent motion patterns (Zeki, 2015). The output from the cells in MT/V5 is then further integrated for additional analysis in the MST (Medial Superior Temporal) area (Mather, 2010; Helfrich, Becker and Haarmeier, 2012). It is also known that there are projections from MT/V5 cells to other areas of the visual cortex for integration of global motion signals such as area V3A (Nakhla et al., 2020), V6 (Pitzalis, Fattori and Galletti, 2015) and strong connections with some regions in the intraparietal sulcus (IPS) (Pitzalis et al., 2019). Thus, this retinal motion information

processing is based on the condition that a population of cells in V1 which are direction-selective detect local motion and project information to the MT/V5 area and which then is integrated to obtain perceptions of global motion (Kaas and Collins, 2003).

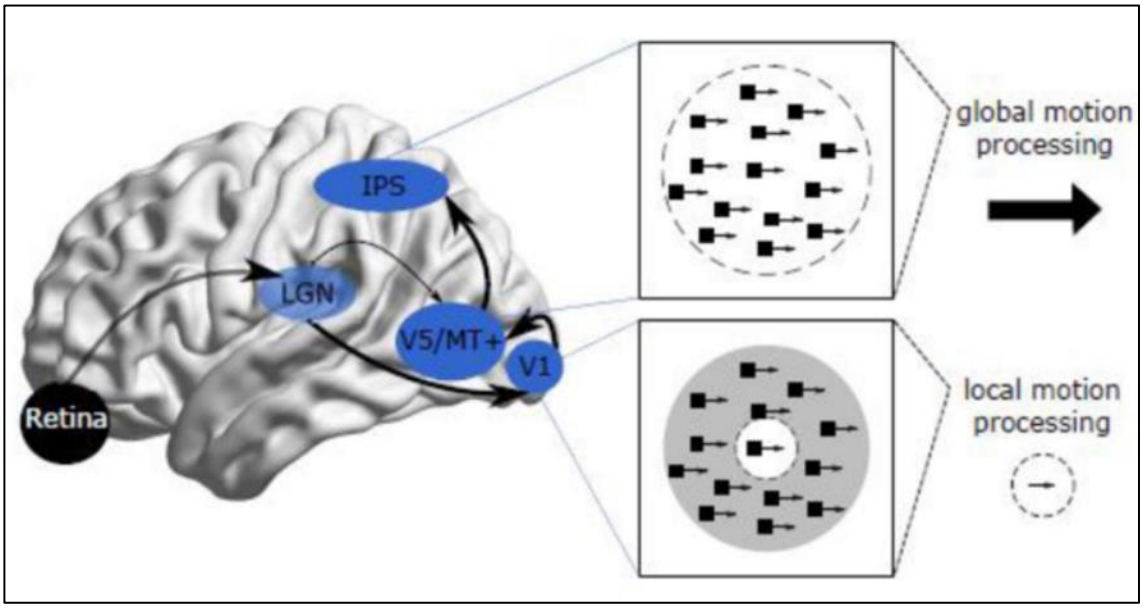

Figure 1.3. Retinal Motion Processing Pathway. The earliest motion-selective cells are within the retina. From there information is relayed upstream to the LGN, which projects mostly to V1 but with some direct projections to V5/MT. V1 also projects directly onto V5/MT, which has dense connections with regions around the intraparietal sulcus (IPS). While V1 neurons have small receptive fields and are thought to represent local motion, V5/MT represents global motion.

In this process of computing global perceptions through local impressions, a problem arises that was first described by Wallach (1935) as the inherent ambiguity of the direction of motion of a line, which later became known as the "aperture problem" (Wuerger, Shapley and Rubin, 1996). The aperture problem consists in the impossibility of assessing the true direction of motion through a simple local projection, whether it is caused by the motion of an object, or a unidimensional feature seen through a small aperture or by the small receptive field of a neural motion sensor (Rider, Nishida and Johnston, 2016).

In Figure 1.4A it is possible to observe how the perception of the direction of motion is influenced depending on the position of the aperture where the one-dimensional

object is visualized. In the top example, we can even understand that the perceived motion direction is different from the true one and remains unchanged whether the line moves upwards or downwards.

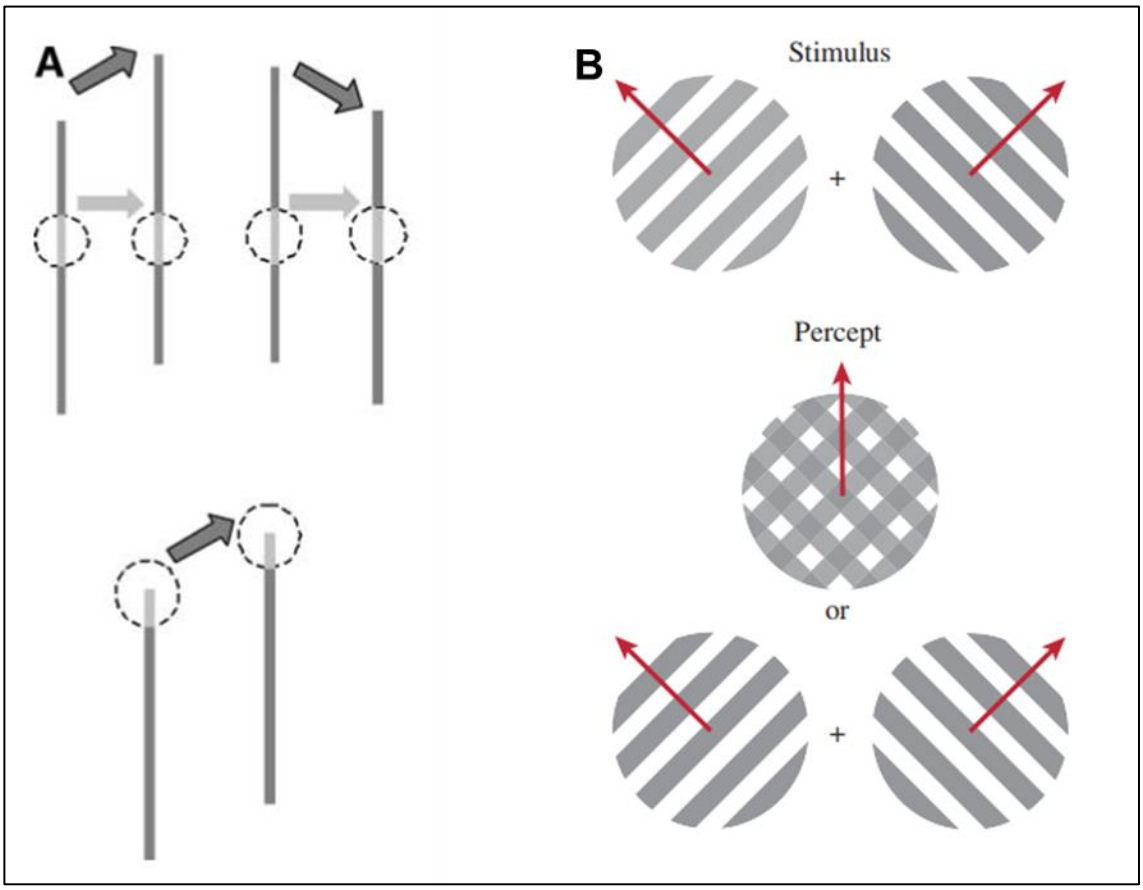

Figure 1.4. Aperture Problem and Ambiguous Motion Stimuli. (**A**) A small aperture (dotted circle) positioned at the center of a moving bar allows detection of only the rightward component of motion (light gray arrow), regardless of the actual motion direction (dark gray arrows). However, an aperture positioned at the endpoint of the bar permits measurement of the correct motion direction. (**B**) Two series of oblique lines (gratings) with orthogonal directions of movements are superimposed ('Stimulus'). The subject may perceive the image ('Percept') as two gratings moving in opposite directions, or as a single cross-hatched object moving upwards (indicated by the arrow). The percept alternates between the two interpretations. Reproduced from (Schwartz et al., 2012; Pack et al., 2003)

Briefly, the problem lies on the shortcomings that the brain has in integrating speed and direction of moving objects (2D) from local projections (1D). These local readings alone are insufficient to determine the true motion of the object (Lorenceau et al., 1993) and as such, several approaches have emerged to try to explain the solution to the aperture problem. There are two categories of models that make similar predictions but differ in the stage at which comparisons between two local measurements take place. The most accepted model, known as the standard, refers that the solution involves the combination of two local signals with different orientations. It is known as integrationist model. Its first stage is the parallel extraction of local motion signals through the cells of V1, which have small receptive fields. In the second stage, these signals are non-linearly combined in regions like MT/V5 and integrated to achieve 2D velocity. In a third, more complex stage in the MST region, the 2D motion vectors are analysed to obtain motion components such as rotation and expansion. The second category of models, the selectionist models, refers that the combination is made in the first stage in the primary visual cortex through End-stopped V1 neurons. These types of neurons are capable of encoding 2-dimensional motion signals into regions of the receptive field that capture parts of the retinal image that contain multiple stimulus orientations. In the second stage, the outputs of the first stage are averaged in order to compute the 2D velocity. In Figure 1.4A, in the example below, when observed through an aperture that contains an endpoint, it is possible to extract the true component of motion of the line (Pack and Born, 2008; Rider, Nishida and Johnston, 2016; Pack et al., 2003; Masson and Ilg, 2010).

One of the main experiments that support integrationist models is the work described in by Movshon and colleagues (1985). It mentions that a contour alone is not sufficient to determine the motion of the object they are inserted in. It features the famous example of the 3 gratings, one that moves diagonally upwards and to the left, another that only moves upwards and a third that moves exclusively to the left. The moving grating is seen in the same way through the aperture, and with the same perception of motion for the 3 cases, with a direction normal to the direction of the

grating's bars, revealing that the different possible interpretations derive from the structure of the stimulus.

When two gratings, which are viewed through the same circular aperture and with mirrored dispositions, are superimposed, they form a visual plaid (Figure 1.4B). Visual plaids are a type of ambiguous stimulus that result from superimposed gratings, with similar frequencies, contrasts and speeds. The visual system, when observing an image of this kind, usually has a preference to perceive a coherent motion, that is, a motion in a single direction in which the resulting movement pattern is the 2D direction intermediate to the two 1D directions of each grating. However, it is also possible to perceive the visual plaid as two gratings that move in opposite directions (Figure 1.4B) (Castelo-Branco et al., 2000; Pack and Born, 2008).

1.2.4. Electroencephalography

Electroencephalography is the study of electrical potentials generated in the brain and captured by electrodes positioned along the scalp. As a rule, this is a non-invasive method and was developed in 1929 by Hans Berger. This German neuropsychiatrist was the first to perform scalp readings of electrical activity in humans (Berger, 1929; Gloor, 1969). This electrical activity is called an electroencephalogram or EEG. The main objective of studies using the EEG is to try to relate the measurements of neural dynamics with a functional brain state, and for this reason it is one of the standard methods still used today to measure neural activity in humans and the main source of signals for non-invasive brain computer interfaces (BCIs) (Müller-Putz, 2020; Srinivasan et al., 2007))

EEG is a unique technique and has obvious advantages because it is able to measure electrical activity from the brain directly, in real time, is non-invasive and relatively inexpensive to perform. These 4 factors make the EEG a helpful tool for clinical diagnosis, more specifically in the field of epilepsy, and scientific research (Kayser and Tenke, 2015).

This direct EEG measurement of voltage modulations picked up by the electrodes reflects the biological and physiological phenomena that take place at the level of neurons within the brain. The brain can be interpreted as a huge neural network, which is interconnected, and divided into many subnetworks. Ionic currents cause changes in extracellular potentials. These changes, which originate from synaptic transmissions and action potentials of neurons, are called local field potential (LFP), which originate from the sum of potentials from several neurons, with a greater contribution from post-synaptic potentials (Buzsáki, Anastassiou and Koch, 2012). The potentials captured in the EEG are slightly different from the LFP, because the attenuation that the potential undergoes from the source to the scalp electrode is sufficient to reduce its intensity and produce a spatial smoothing that occurs due to the conductance of brain tissues (Müller-Putz, 2020). The greater the synchronous activation of cortical neurons, the greater the modulation of local potentials, which in turn produce higher amplitude signals on the EEG (Schomer and Lopes, 2012). The EEG allows for the study of neurocognitive processes that happen in tens or hundreds of milliseconds, whether they are cognitive, linguistic, motor or perceptual processes. The events that trigger them can also extend from milliseconds to seconds. As such, a high temporal resolution technique is needed to achieve these fast, dynamic and sequential events as is the case with EEG. Another advantage of this technique is that the signal from the EEG is multidimensional, encompasses time, space, frequency, power and phase. All this range of information available in a single signal allows analysis of different aspects of brain activity, testing different hypotheses and possibilities for neuronal processes (Cohen, 2014).

The continuous recording of the EEG signal is the measurable part of the cerebral electrical activity that is maintained in a living individual, and as such, a large part of the signal originates from rhythmic oscillations that can be smaller than 1 Hz and reach values up to 100 Hz (Müller -Putz, 2020). These oscillations observed in the EEG data are a direct reflection of the neuronal oscillations that take place in the cortex. The neurophysiological mechanisms responsible for these large-scale oscillations can have different origins and are modulated according to the frequency bands they belong to (Buzsáki and Wang, 2012; Wang et al., 2012). Brain rhythmic

activity contains simultaneously several frequencies, which can be separated through digital processing techniques, and are organized into frequency bands: Delta with 1-4 Hz, associated with deep and unconscious sleep states; Theta with 4-8 Hz, related to states of sleep and drowsiness; Alpha with 8-13 Hz, characterized by states of relaxation in awake individuals with eyes open; Beta with 13-30 Hz, linked to mental activity such as attention, anxiety and vigilance; Gamma with 30-200 Hz, associated with arousal and perceptual binding mechanisms (Müller-Putz, 2020; Purves, 2018; Cohen, 2014). Nonetheless, the sources of many of these oscillatory signals are currently unknown, the functions of each band go far beyond those described and a definite role for each is still under debate. Still, there are no well-defined limits to the oscillations because there is no universal scientific consensus.

In these continuous EEG measurements, the electrodes' positioning plays a key role in localizing the electric fields that reach the scalp. Taking into account that the location can always have some influence on the detection and classification of brain activity, it allows the electroencephalographer to determine whether the activity really had a brain origin or if it was nothing more than an artifact. The interpretation of an EEG in a clinical setting also depends on the cortical location of the EEG recordings. As such, several methods were devised to obtain a standardization of electrode placement. The 10-20 electrode system is the *de facto* standard used in clinical EEG studies (Jasper, 1958). In this model, electrodes are placed at distances of 10% and 20% of 4 anatomically defined points. It allows to position up to 21 channels. With the improvement of technology and new multichannel hardware for EEG to obtain greater spatial resolution, a new method based on the previous one was introduced to increase up to 74 electrode positions and thus be able to make comparisons between studies that used the 10-20 system (Chatrian, Lettich and Nelson, 1985). It is called extended 10-20 system or 10-10 system (Figure 1.5) and uses proportional distances of 10% between anatomical points. In an even more advanced way of presenting a standardization of electrode location for studies involving high spatial resolution and well-defined neuroimaging data, the 10-5 system or 5 % system (Oostenveld and Praamstra, 2001) appears, with a similar positioning method to the 10-10 system but with distances of 5% and 345 possible positions.

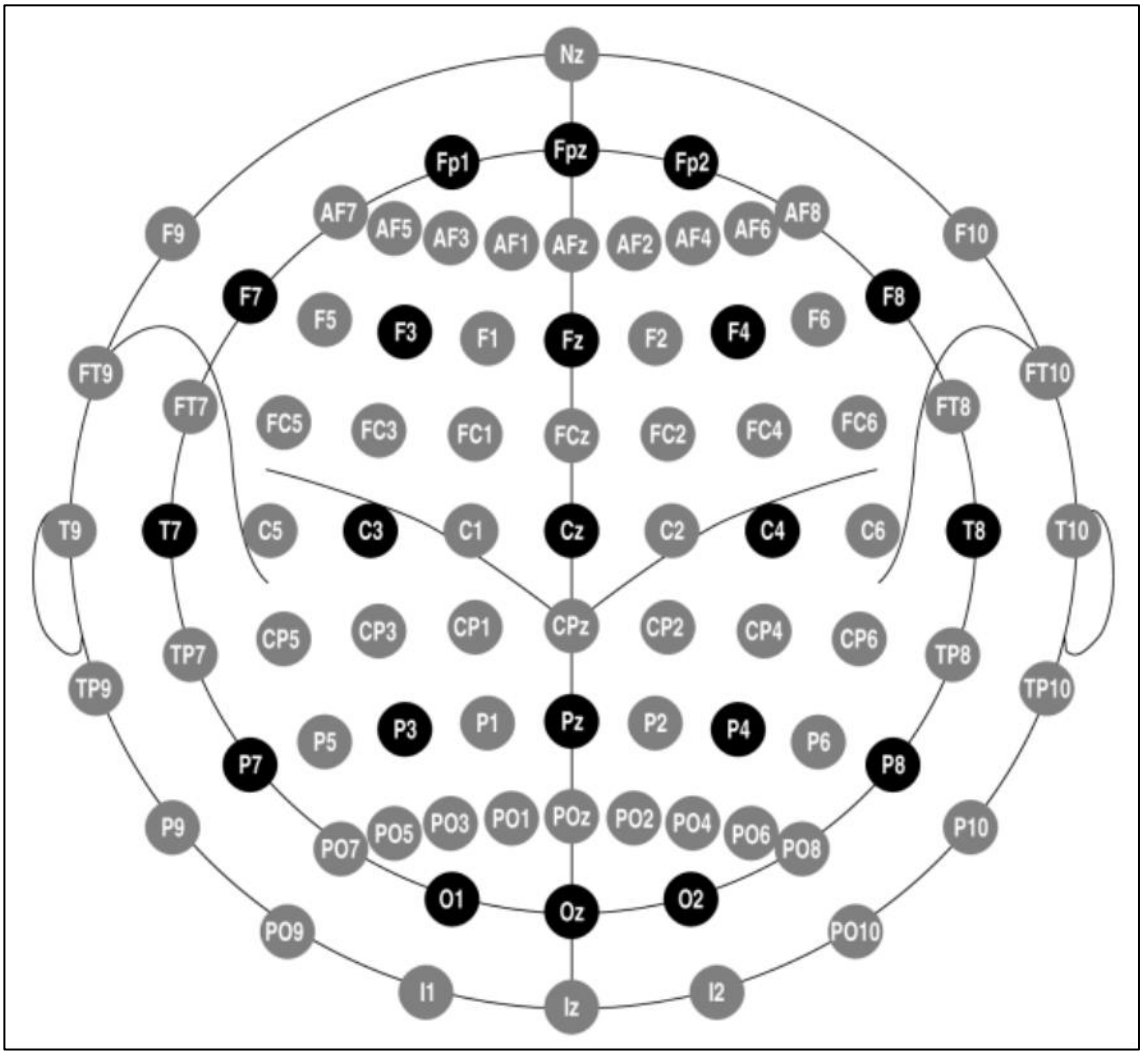

Figure 1.5. The 10-10 Electrode Positioning System. Electrode positions and labels in the 10-20 system. Black circles indicate positions of the original 10-20 system, gray circles indicate additional positions introduced in the 10-10 extension. Reproduced from Oostenveld and Praamstra (2001)

The measurement of EEG recordings is voltage, microvolts (μV) are typically used more often, as the electrical activity captured at the scalp level is of a very low order of magnitude. However, for the EEG the microvolts are relative values, this due to the fact that the measurement of each electrode is the difference between the potential measured in that same electrode and a reference electrode positioned in another location of the head (Cohen, 2014; Nunez and Ramesh Srinivasan, 2006). This fact presents itself as a limitation of the EEG, as it makes it a technique dependent on the choice of reference, which alters the voltage values and reflects in all electrodes some activity present in the reference electrode.

1.2.5. Event-Related Potential

Despite the advantages and flexibility of EEG it is still a technique with several shortcomings, mainly in the form of being equally sensitive to actual brain activity as to artifacts that result in scalp and head potentials but are unrelated to brain signals. As such, methods have been devised of rescuing true brain signals using data pre-processing (i.e., filtering, artifact removal) and averaging of several repeated events. It is possible through averaging techniques to increase the signal-to-noise of a particular brain response and extract from the EEG brain activity resulting from exposure to sensory stimuli or cognitive events. The potentials that are generated because of these specific responses are called event-related potentials (ERP) (Luck, 2014).

ERP analysis is the process of examining changes in the brain's electrical activity timelocked to a specific stimulus and averaged across trials. The objective is to analyse and identify changes in cortical potentials that are specific to the stimuli being presented. ERPs are thought to reflect specific cognitive and perceptual processes that occur in the brain in response to a particular event. For example, when a person sees an object or hears a sound, their brain responds with a specific pattern of electrical activity that can be measured using EEG.

ERP analysis typically involves several steps, including data pre-processing, epoching, averaging, and statistical analysis. During data pre-processing, the raw EEG data is cleaned and organized in preparation for analysis. Epoching involves dividing the EEG data into segments, or epochs, that correspond to specific events. The averaging process involves taking the mean of multiple epochs to create a more stable and reliable measure of brain activity, meaning that each channel has only one average trial for each subject.

According to Regan (1989), an ERP reflects a true response if the brain mechanisms relevant to the event are in resting states before the stimulus and return to these same states before the next stimulus. Historically, ERPs only started to be characterized 35 years after the first EEG was performed in humans. Contingent Negative variation (Walter et al., 1964), visual evoked potentials (Cooper et al., 1965), mismatch

negativity (Näätänen, Gaillard and Mäntysalo, 1978), P300 (Sutton et al., 1965), N400 (Kutas and Hillyard, 1980) and N170 (Bentin et al., 1996) are some examples of the most known and studied components and potentials in ERP analysis.

An ERP has several advantages, but it is necessary to understand the type of questions that this technique is capable of answering. First, it is easy to compute and requires few parameters for comparing the brain processing that takes place when a subject is exposed to two types of conditions. Second, it inherits an advantage of the EEG, which is the high temporal resolution, because it allows showing with high precision the moment in which the stimulus is processed in the cortex and the state of the brain before, during and after the stimulus. Third, there is an extensive literature available on ERPs that allow comparisons to be made and results evaluated. Lastly, ERPs offer good evaluation of single-subject data (Luck, 2014; Cohen, 2014; Luck and Kappenman, 2011).

But an ERP study also has its limitations. It lies mainly in the fact that the potentials recorded on the scalp are nothing more than the sum of several components generated in the brain and therefore becomes very difficult to decompose this mixture and individualize each component. Another known limitation is the lost information related to the event when performing an averaging process. It may even give rise to components that are unrelated to the event (Nikulin et al., 2007).

1.2.6. Oscillations and Potentials in Ambiguity/Perception

The neural networks that make up the human brain show rhythmic fluctuations in the excitability of sets of neurons. These oscillatory bands can range from 0.5 to 100 Hz. Neighbouring frequency bands can be associated with different brain states and responses, but they can also temporarily coexist and be activated by the same cortex zones and interact with each other to form complex oscillatory activity (Engel, Fries and Singer, 2001; Csicsvari et al., 2003; Kopell et al., 2000; Buzsaki, 2004).

When there is a bistable perception, the subject alternates between perceptions, but in the periods between these perceptual switches, perception remains stable until the event of the next exchange. Recent studies indicate that the power and frequency of alpha oscillations play a role in mediating this perceptual stability (Katyal et al., 2019; Piantoni et al., 2017; Zhu, Hardstone and He, 2022). These findings report that with increasing alpha power, the duration of perception of a stimulus configuration is prolonged, which leads to the conclusion that greater activation of these waves promotes perceptual stability. In the moments that involve the perceptual change, Strüber and Herrmann (2002) report that there is a constant alpha power that suffers an abrupt drop 300 to 200 msec before the button-press in an exogenous reversal and 1000 msec before for an endogenous reversal. İşoğlu-Alkaç and Strüber (2006) also describes that this decrease in alpha waves before the perceptual change has a higher incidence in the lower alpha bands.

Beta oscillations also play a role in visual perception. Okazaki et al. (2008) demonstrated with a bistable figure that 250 to 450 msec from when there is a perceptual switch to a dominant and more stable configuration of the visual stimulus there is greater activation of betas, with higher incidence in the parietal and occipital regions, when there is a perceptual switch to a certain configuration of the visual stimulus, which is considered dominant and more stable. Piantoni, Kline and Eagleman (2010) reveal that there is a greater activation of beta waves in perception of real motion than when perceiving an illusory motion of bistable figures, however, at the moment of the perceptual change, the power was similar for both conditions. Zaretskaya and Bartels (2015) used a bistable stimulus with either local motion or global motion settings. They describe how there is a decrease in the power of the betas when the subjects perceived a global motion in relation to the configuration with local motion. Although the authors state that beta waves play a role in motion integration, there is another possible interpretation that is related to the fact that the first perception is local motion and betas play a role in the dominant or default interpretation. This idea is also supported by the hypothesis proposed by Engel and Fries (2010), where they conjecture that the activity of beta waves is related to the maintenance of the current sensorimotor cognitive state, that is, beta oscillations are

more active if the maintenance of the cerebral status quo is intended rather than a change of that state. Costa et al. (2017) demonstrates that there is also a greater activation of the betas when the perception shifts to a more stable configuration of a bistable figure with ambiguous motion, though in this study the more stable stimuli also correlates with a bound/global motion configuration. It is also known that when there is movement production, normally the report through a button-press, there is an attenuation of the power of the betas, which is followed by a rebound to stable values when this movement production ends (Heitmann, Gong and Breakspear, 2012).

For the gamma frequency range, Başar-Eroglu et al. (1996) found an enhancement for the gamma band with 1000 msec before the key press related to dynamic ambiguous stimulus pattern reversals compared to periods of perceptual stability. In Mathes et al. (2006), subjects had to voluntarily accelerate or decelerate the reversal rate or maintain a passive attitude towards a stimulus from a Necker cube. The study states that there is a greater activity of gamma waves during the deceleration condition. In short, gamma waves seem to show greater activity in a 1000 msec interval before reversals of ambiguous stimuli (Kornmeier and Bach, 2012).

Regarding the potentials, about 250 msec before the key press, there is a positive ERP located in parietal electrodes with motion direction reversals of a stroboscopic alternative motion stimulus (Başar-Eroglu et al., 1996) and with orientation reversals of Necker's cube (Strüber et al., 2001). This parietal positivity is considered as a variant of the P300 component. A relationship was found between reversals and parietal positivity, which assumes that this occurs with motion reversal and reflects conscious recognition.

1.2.7. Models to Explain Oscillations and the Generation of cortical Potentials

The potentials generated by the cortical mechanisms, and which are captured in EEG investigate and understand the processing of stimuli and the inner workings of the human brain. As already described, ERPs are calculated by averaging EEG data time-locked to an event that happens many times. These types of potentials are

composed of slow and fast components. These slow components can last hundreds of milliseconds and are related to several cortical mechanisms such as working memory (Vogel, McCollough and Machizawa, 2005) or action monitoring (Kilner et al., 2004).

The oscillatory activity of the EEG can assume different frequency bands and is related to the subject's perception. These relationships are described in the section above. However, several studies point to a correlation between ERPs and brain oscillations. Examples of this relationship is the study by Wang et al. (2012), which demonstrates a functional association between beta oscillations and the N400 component involved in language comprehension, or the theta and delta activity being related to error-related negativity (Yordanova et al., 2004) and the P300 (Rangaswamy et al., 2007).

Nonetheless, typically oscillations and ERPs are not studied together, and some argue that the two phenomena were unrelated, because ERPs are generated by additive evoked responses, which is totally independent of continuous oscillations (Mäkinen, Tiitinen and May, 2005; Shah et al., 2004). However, in a completely different view, Hanslmayr et al. (2007) and Makeig et al. (2002) state that ERP emerge exclusively from the phase resetting of oscillations. However, it is possible to interpret the results from a neutral perspective, that is, in a position where it is considered that the oscillatory activity affects ERP generation and influences its amplitudes, but it is not the singular cause that gives rise to the potentials.

There are few models capable of explaining how the modulation of brain oscillations generates slow components in ERPs. It is a field of electrophysiology that deserves further investigation. The first category of models, that is sometimes described as "additive model", states that ERPs and EEG are neuronal events completely independent of each other and that the stimulus is a phase-locked additive response in each trial. When averaging across trials, all oscillatory activity that is not phase-locked to the stimulus is eliminated and only the components related to the evoked response remain (Bastiaansen, Mazaheri and Jensen, 2011).

Another type of models is the so-called phase-resetting model, which states that EEG and ERPs are the same neuronal event, and the components originate from a superposition of EEG activity that resets its phase and becomes aligned in response to

the stimulus. The resetting of the phases after averaging the trials causes a slow component, visible in the ERP waveform (Figure 1.6) (Bastiaansen, Mazaheri and Jensen, 2011; Sauseng et al., 2007).

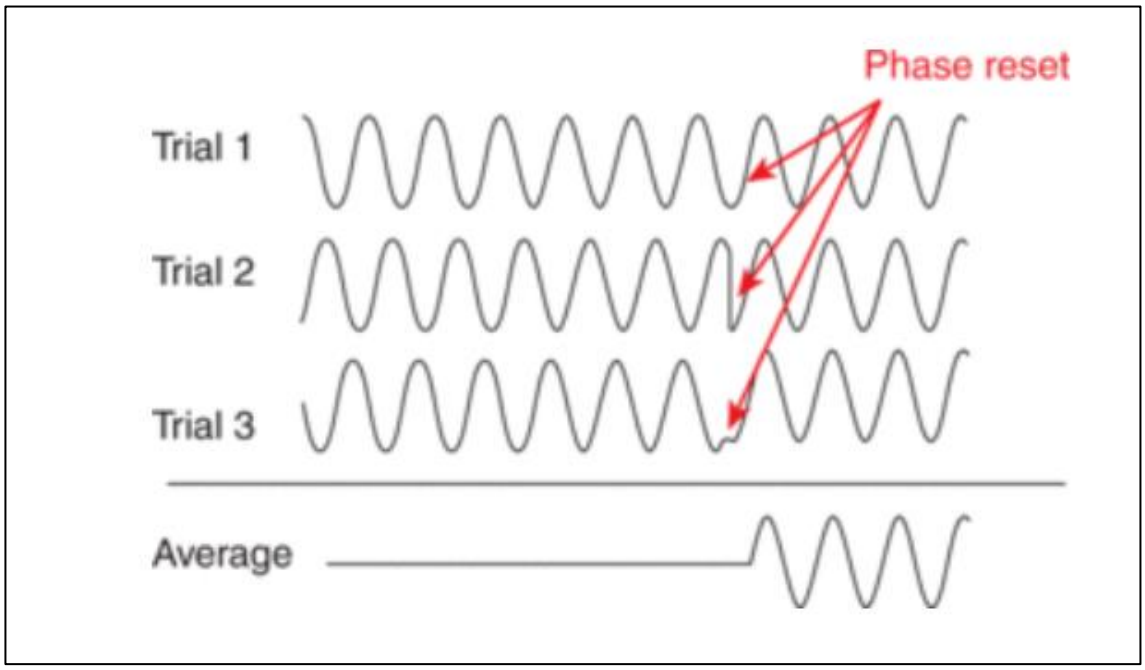

Figure 1.6. Fundamentals of Phase-Resetting Model. Simulated data illustrating the principle of phase resetting. Three single trials are shown whose phases are not aligned initially. Red arrows indicate the point in time at which an event-induced phase reset occurs. The bottom trace shows what the average ERP would look like if a sufficient number of such trials (in practice >30 trials) are averaged. (Reproduced from Bastiaansen, Mazaheri and Jensen (2011)).

In order to understand how the EEG data are related to relevant stimuli or tasks, the analysis of ERPs or the modulations of the oscillatory activity itself coming from the subject's scalp can explain the response coming from that same stimulus. As an alternative to these two types of models, a new one has been described that addresses the relationship between ERP and brain oscillations in a completely different and innovative way. It was defined by Mazaheri and Jensen (2008) and proposes hypotheses for both electroencephalography and magnetoencephalography (MEG). They describe that the oscillatory activity of EEG can explain the generation of slow

components in the ERPs measured through the EEG. These slow components can last hundreds or thousands of milliseconds and can be a consequence of the asymmetric modulation of brain oscillations, which when an event-related averaging is performed, gives rise to a negative shift in the ERPs when the peaks are more modulated or a positive shift when the troughs have greater modulation (Figure 1.7). The analysis of the modulations of the oscillatory activity is done through the asymmetric fluctuations in the amplitude of peaks and troughs of the EEG signal with the help of an index and a mathematical formula described in Mazaheri and Jensen (2008).

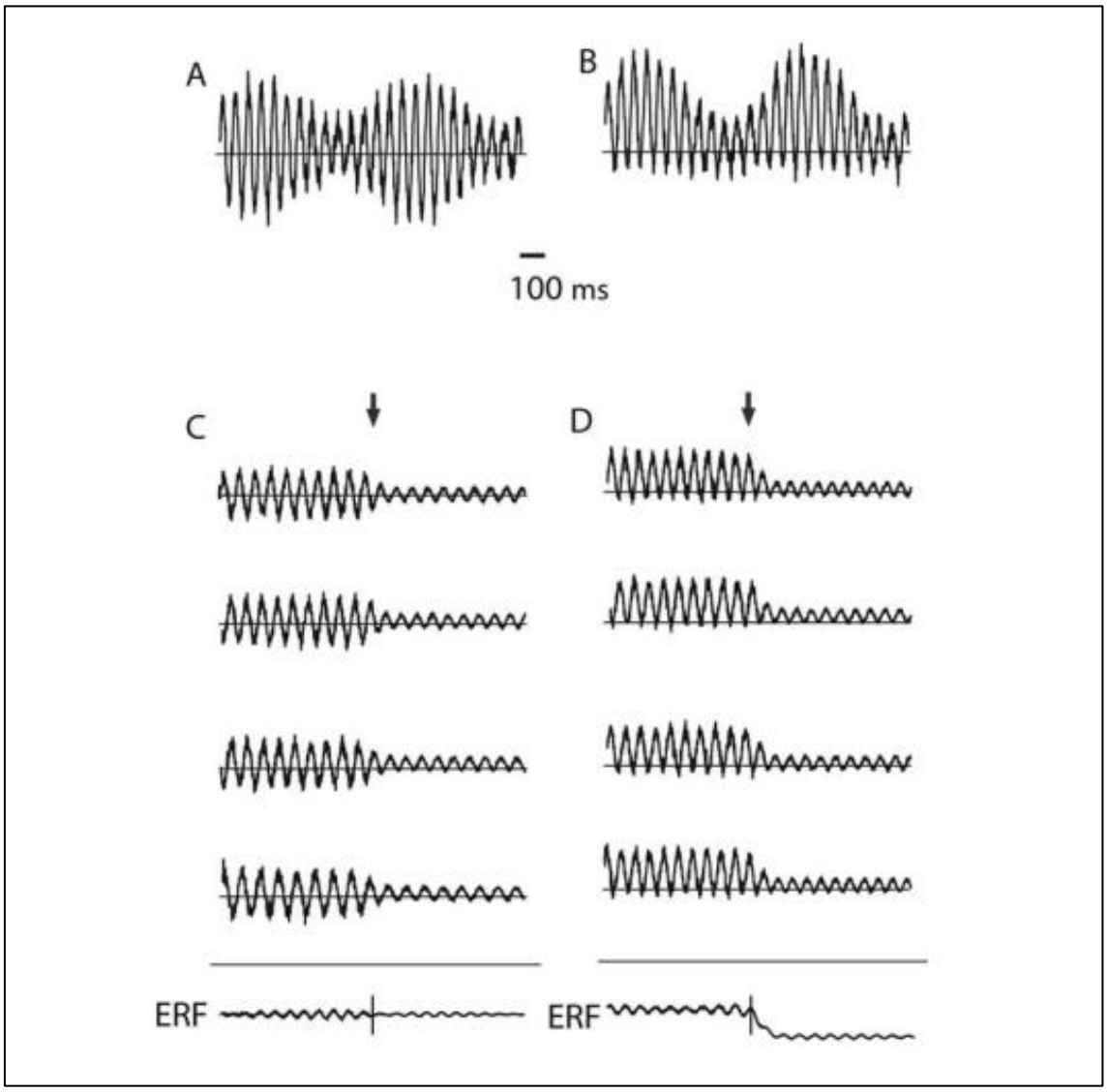

Figure 1.7. Asymmetric Amplitude Modulation of Oscillations and Its consequences on ERPs. (**A**) The amplitude modulation of neuronal oscillatory activity is conventionally viewed as being symmetric at approximately zero. (**B**) The amplitude modulations of the oscillatory activity are asymmetric such that the peaks are more strongly modulated than the troughs (or vice versa). (**C**) The conventional view ignoring asymmetric modulations of oscillatory activity would mean that averaging across trials (the arrow representing the start of the evoked response) would not result in the generation of slow fields. (**D**) As a direct consequence of amplitude asymmetry, a depression (or increase) in alpha activity in response to a stimulus will result in the generation of slow fields when multiple trials are averaged. Reproduced from Mazaheri and Jensen (2008).

1.3. Work Goals

This work addresses different aspects of electrophysiology. Topics and concepts involving the perception of bistable motion stimulus and how electroencephalography proves to be a capable technique to understand the cortical mechanisms behind the resolution of visual ambiguity are addressed. This work performs two types of analyses that are conventionally not carried out together, although there are current efforts to combine information from ERP analysis and time-frequency analysis (Tamura et al., 2012; Marturano et al., 2020). Hereby, the objectives of the work are:

- To study the mechanisms and potentials that are involved in the visual processing of an ambiguous stimulus as well as the regions where they are generated;
- To understand the influence that the oscillatory activity of the brain has on the perceptual change and which frequency bands have greater activation for this process;
- To find a connection between the cortical potentials that are evoked by the perceptual exchange event with brain oscillations;
- To investigate if the model of asymmetric amplitude of oscillatory activity explains the generation of slow components of the ERPs;

2. Methods

In this chapter, it will be presented all the methods executed in the experimental part of the work. The EEG dataset used were the same acquired in the study by Costa et al. (2017).

2.1. Participants

The group of participants consisted of 12 women and 9 men, making a total of 21 participants, all healthy and aged between 22 and 36 years. They were students or staff at the University of Coimbra. All had corrected-to-normal vision and were right-handed. All procedures were performed in accordance with the Declaration of Helsinki and approved by the ethics committee of the Faculty of Medicine of the University of Coimbra. Participants gave their written informed consent before the activity.

2.2. Stimulus

The stimulus consisted of angled lines that meet in the center of a white rectangle, with an orientation of 45° in relation to the x-axis, for the image on the left side and 135° for the one on the right side. The stimulus describes a movement speed of 5°/sec and a size of 10° x 11° (vertical and horizontal respectively). A blue cross of 0.4° was used as a fixation point. The stimulus viewing distance was 70 cm and presented on an LCD with a refresh rate of 60 Hz. The stimulus and the experiment were created in MATLAB, using the Psychophysics Toolbox (Brainard, 1997), as in Costa et al. (2017) (see Figure 3.1 for stimulus visualization).

2.3. Experiment

EEG data were acquired while participants observed the ambiguous stimulus for 3 minutes repeating that task 8 times, maintaining visual fixation on the central blue cross, reporting the perceived movement by pressing and holding a button for when they perceived a "Bound" configuration, with a downward movement spanning the entire stimulus which was perceived as a single texture, and another button for the perception of a "Unbound" configuration, with an inward movement and an illusory separation of the left and right halves of the stimulus that appeared segregated. In case of doubt by the participant, it was also possible to abstain from reporting by not pressing any of the buttons. The button-pressing was conducted with the right hand on one half of the experiment while the other half used the left hand. Although there may be different perceptions from those described above, these were rarely or practically never reported by the participants in this experiment, based on assessments during pilot studies and also after participants were debriefed. For the purposes of the previous study (Costa et al 2017), the alternative perceptions could be categorized as "Unbound", because the clear separation that occurs in the middle of the stimulus is an inherent characteristic of all and easily identifiable by the participants. These criteria were also employed here.

2.4. EEG Acquisition, Pre-Processing and Analysis

Data were recorded using a 64-channel system (Easy-Cap, Munich, Germany), with 58 Ag/AgCl electrodes placed according to the extended 10-20 system. Signals were acquired at 1000 Hz, amplified and lowpass filtered at 200 Hz. All the electric impedances were kept lower than 10 kΩ. Data were later analysed offline using MATLAB (The MathWorks, Inc., Natick, MA, version R2019a) and EEGLAB (Delorme and Makeig, 2004). In this initial phase of analysis in EEGLAB, the datasets were firstly downsampled to 500 Hz, a baseline of -500 to 0 msec was applied in relation to the trigger that indicated the beginning of the visual task, the periods containing artifacts were removed by visual inspection. In case of bad channels, these

were interpolated using a spherical spline interpolation. The data was then bandpass filtered from 0.1 to 100 Hz. Independent component analysis was computed on datasets highpass filtered at 1Hz and the computed weights were used to remove components identified as artifacts on the original bandpass filtered (0.1 to 100 Hz) data. Blinks, eye movements, and other artifacts were further removed by excluding epochs with amplitude exceeding ±100 μV within a ±1500 msec window from motor response for timelocked epochs. For stable periods the same amplitude threshold was used for events around the full time windows, i.e. from 0 to 1000 msec. The datasets were then exported to the FieldTrip Toolbox (Oostenveld et al., 2011) for filtering, plotting, statistical and timelocked analysis. The data was also re-referenced using average reference and reference-free method Surface Laplacian/Current Source Density (CSD) (Kayser and Tenke, 2015) using the FieldTrip toolbox, meaning that it was made always an analysis for each type of reference and a comparison between both.

2.5. Independent Component Analysis

Independent component analysis (ICA) is a tool that allows the unmixing of different sources that are linearly combined, i.e., it allows you to recover individual components when the only information available is a complex mixture of data. In the case of EEG, which consists of a complex set of signals and potentials originating from different regions of the head, the ICA presents itself as a useful instrument to recover information and refine the EEG signal from true cortical sources. This method also allows one to achieve a greater understanding of the different sources of that same EEG signal (Stone, 2002).

For this study, the ICA was used to identify sources of noise which affects the EEG signal and to remove them, in a crucial clean-up step in the pre-processing pipeline, using infomax algorithm. This calculation was done through the EEGLAB toolbox using the *pop_runica* function on data that had been highpass filtered from 1Hz and then applied to the data that were to be analysed, which was filtered at 0.1-100 Hz.

The reason for not doing the ICA straight away on data with a low highpass filter, i.e., below 1 Hz, served both as a way to achieve a quicker ICA computation but also as a method to obtain more physiologically relevant components, thus excluding slow fluctuations and trends unrelated to the dynamics of cortical activity. It should also be noted that the ICA weights were exported to data with the same number of channels and the same reference, and it was confirmed that the component activations corresponded to expectations.

Finally, the ICA components that corresponded to noise from eye movements and blinks were removed through topographical analysis of the scalp and its power spectrum.

2.6. Filtering

In the EEG acquisition, the data were filtered by a lowpass FIR filter at 200 Hz so that EEG recordings with a frequency band of interest were not lost, but also to prevent the phenomenon of aliasing. This is a phenomenon that generates artefactual signal at a lower frequency when the EEG signals are recorded with a frequency below the Nyquist frequency, which is half the sampling frequency (Epstein, 2003). The data was thus recorded with a sampling rate of 1000 Hz and all EEG signals with 500 Hz or more would suffer the consequences of aliasing and be represented into lower frequency artifacts. To avoid this effect, a 200 Hz lowpass filter was applied at the time of acquisition and prior to the signal being digitized.

Midway of the pre-processing in EEGLAB toolbox, the data were filtered with a bandpass FIR 0.1-100 Hz using the *pop_eegnewfilt()* function. This frequency band allows the main oscillations that exist in the EEG signals, like the delta, theta, alpha, beta or gamma waves, to be maintained in the signal and also allows one to perform ERP analysis that often shows important signal components with slower time-dynamics, below 1Hz. Afterwards, using the FieldTrip toolbox the data was lowpass FIR filtered at 30Hz using the *ft_preprocessing* function for the ERP analysis. ERPs capture mainly phase-locked activity, which is absent or vastly reduced in frequencies

above 30 Hz. More specifically for the interests of the current study, potentials originating from oscillatory activity within the alpha and the beta bands (8 to 12 Hz and 13 to 30Hz respectively) were maintained.

2.7. Epoch Selection

Two epoch selections were made: one to represent moments of perceptual transition to either configuration and another to represent stable periods of Bound and Unbound perceptions.

2.7.1. Perceptual Change Epochs

For the epochs of perceptual change, a time window of ±2500 msec was defined, centered on the 0 msec timepoint, corresponding to the press of a button representing the perceptual change for the subject. This selection results in two types of epochs: one that represents the transition to a Bound perception and another to an Unbound perception. All epochs that did not meet this time window criteria or that contained artifacts were completely ignored and removed.

The epochs containing the perceptual change are thus timelocked to the motor report and can correspond to a perceptual switch from Bound-to-Unbound (BU) or from Unbound-to-Bound (UB).

2.7.2. Stable Perception Epochs

Epochs of stable periods of perception were obtained via continuous EEG signal not including 250 msec before and after pressing a button, i.e., the acquired data that was recorded in between different perceptual shifts excluding a 500 msec window around a perceptual change. These epochs last for 1000 msec, are nonoverlapping and

represent only one type of perceptual configuration: Bound (SB) and Unbound (SU).

2.8. Data Referencing

The data acquired through the 64-channel system had the CZ channel as reference (Extended 10-20 system) during online visualization and digitization. It is noted that, when working with EEG signals, the use of a reference that is constant or zero in order to have the least impact on the study can be something utopian, which is why there is always the problem of knowing which reference is most suitable for each case (Yao et al., 2019). In this work, this problem also arose and had a great significance in the outcome of our analysis and consequently in our conclusions. As such, it was decided to evaluate two types of reference: a unipolar reference (Average Reference) and a non-unipolar reference (Surface Laplacian/CSD Reference-free method).

The Average Reference was obtained through an offline calculation of re-referencing completed in the EEGLAB toolbox (*pop_reref* function) and considered as one of the best options due to the theoretical conception that the dipolar nature of the components existing in the ERPs implying that superficial sources will produce equivalent positive and negative potentials distributed across the scalp. In other words, this re-referencing method assumes that the sum of all potentials across the entire scalp is equivalent to zero (Luck, 2014). However, it has already been proven that this concept is not entirely true by Yao (2017), since the integral of the EEG potentials for a shape similar to a human head is not zero, but even so the Average Reference presents itself as an option widely used and accepted by scientists.

For this reason, another type of reference was used, the Surface Laplacian/CSD, and was obtained using Fieldtrip toolbox routines (*ft_scalpcurrentdensity* function). This function is based on the formula of Surface Laplacian of voltage Φ recorded on a plane surface with coordinates (x, y):

$$Lap = \frac{\partial^2 \Phi}{\partial x^2} + \frac{\partial^2 \Phi}{\partial y^2}$$

It was computed, using FieldTrip and the spline interpolation method (Perrin et al., 1989), an estimate of the scalp current density (SCD) through a second-order derivative (Surface Laplacian) of the EEG potentials distribution. The SCD is a mathematical algorithm that transforms these potentials into estimates of radial current flow along the scalp and if these estimates are positive, it means that the current flow is going from the brain to the scalp and if they are negative the opposite happens (Kayser and Tenke, 2015). Most importantly, one should remember that all estimates calculated using this algorithm are reference free.

2.9. Timelocked Analysis

The epochs referring to the periods of perceptual change were selected based on response-related triggers, i.e., button presses, and all remaining trials after artifact rejection (see Pre-processing section) were averaged in an Event-Related Potentials (ERP) analysis.

The ERPs were obtained using a function *ft_timelockanalysis*, which computes the average between trials and in order to obtain an ERP of each channel of each subject. An average ERP was calculated using the function *ft_timelockgrandeaverage* to have an average ERP over multiple subjects.

Statistical tests were computed to assess differences between the two UB and BU conditions (see Statistical Analysis section). Topographies were plotted with the statistical masks applied in the ERPs. Upon further inspection, we selected a group of channels located in the parietal and occipital region of the right hemisphere of the head and calculated a new mean ERP for these channels. Again, statistical tests were performed for each channel for differences between the two conditions UB and BU and for two latency periods: from -1500 to -300 msec and from 100 to 1300 msec. This two latency periods were chosen because they represent moments of different observed activity.

2.10. Time Frequency Analysis

A time frequency analysis of the EEG data was computed only for the BU and UB epochs with average reference, to evaluate the event-related spectral changes between the two configurations. A multitaper analysis over sliding windows were used for a time-frequency decomposition. The signal was convolved with a sequence of Slepian tapers, the number of tapers provided a balance between temporal and frequency resolution across the spectrum.

This analysis was achieved using FieldTrip's *ft_freqanalysis* function, *dpss* methods, with a frequency of interest from 6 to 60 Hz and a time window of -2.5 to 2.5 sec.

2.11. Asymmetry Analysis

To measure the asymmetry of the oscillatory activity of the human brain, a procedure adapted from Mazaheri and Jensen, (2008) was used. The Amplitude Fluctuation Asymmetry Index (AFA_{index}) is computed through an estimate that relates the variance of the peaks and troughs of the EEG signal. The formula used is:

$$AFA_{index} = \left| \frac{Var(S_{peaks}) - Var(S_{troughs})}{Var(S_{peaks}) + Var(S_{troughs})} \right|$$

S_{peaks} means peaks values of EEG signal and $S_{troughs}$ means troughs values of EEG signal. It was calculated using the EEG time series and custom functions in MATLAB. To obtain a specific asymmetry value for a given frequency band of interest, a bandpass filter is applied to the original EEG data and the timepoints of the peaks and troughs of the filtered data are collected. Then these timepoints are used to obtain the peak and troughs signal values in the raw data. These values are then applied to the formula to calculate the AFA_{index}. The AFA_{index} is a measure that varies from 0 to 1, where 0 represents a symmetric signal and thus its amplitude is modulated in the same way for peaks and troughs and 1 represents a totally asymmetric signal and the variance of peaks is higher than troughs or vice-versa. In its original conception the AFA index could also take a negative value until -1, which means that the troughs have a higher

modulation than peaks, but for the purposes of testing the current hypothesis, only absolute values were used.

2.11.1. AFA Index on Simulated Data

In order to test and understand whether the AFA_{index} estimation was properly implemented and whether it was a good measure to verify the asymmetry of the oscillatory activity in the EEG, simulated data was computed through the FieldTrip toolbox with a deliberately asymmetric configuration. The simulated data were composed by an asymmetric wave equation:

$$A(t) \cdot (1 + \sin(2\pi f t + \varphi)$$

where f is 10 Hz, φ is the random phase value that can assume a number between 0 and 2π, A(t) is a function of amplitude based on a sigmoid:

$$A(t) = a - \frac{b}{1 + e^{t/0.2}}$$

Two conditions were created, the first where the amplitude function was modulated in a decreasing way along the time window and the second in an increasing way. For each condition, 100 trials were created with a duration of -2000 msec to 2000 msec, where 0 is the midpoint of the amplitude function and each trial had the addition of white noise and a random phase. The simulated data were filtered to the frequency band of 8-12 Hz and the timepoints of the peaks and troughs of the filtered data were applied to the simulated raw data for the calculation of the AFA_{index}. An AFA_{index} value was calculated for each trial and then an average value was obtained. This procedure was based on the one used in Mazaheri and Jensen, 2008.

2.11.2. AFA Index on Experimental Data

With the purpose to estimate the asymmetry of the oscillations during periods of perceptual changes and to try to understand how this same asymmetry can be related to the slow components present in the ERPs of the EEG data, the AFA_{index} was applied to these data after all the pre-processing. Epochs BU and UB were used, but only those that had been re-referenced using the Surface Laplacian/CSD reference-free method. The frequency band chosen was 13-30 Hz and was isolated using bandpass filter to that frequency band, as the objective was to understand whether beta waves (13-30 Hz) and their asymmetry were responsible for the slow responses of oscillatory activity in the human brain. They were calculated again by replicating the method used in the simulated data and obtained firstly, an average value of the trials for each channel in each subject, and then an average value only for each channel. A graph was also made that demonstrates the peak-to-peak and trough-to-trough variance for a given set of channels over these same epochs in order to give another view on how these variables behave along the time window encompassing perceptual switch events.

2.12. Non-Timelocked Analysis

The epochs that represented stable periods of perception (SB and SU) were analysed similarly to the epochs that involved a perceptual exchange. They underwent an averaging across trials and across subjects, in order to obtain an average of the potentials for each channel. A statistical test was performed to evaluate the statistical differences between the Bound and Unbound perceptions and the topographies that represented these differences and an average time course of the selected channels P2, P4, P6, P8, PO4, PO8, O2 were plotted.

2.13. Statistical Analysis

To assess the statistical differences between the UB and BU conditions, several statistical tests were performed, for statistically significant differences between two ERPs in a defined time window and in specific latencies. It was decided to use a baseline of -500 to 0 msec defined in relation to the trigger that indicated the beginning of the visual task. This statistical analysis was performed using the FieldTrip toolbox with the *ft_timelockstatistics* function, which provides a robust nonparametric cluster-based test of dependent variables (Maris and Oostenveld, 2007). Critical T-Values from neighbouring points (i.e., time or space/channels, in the case of ERP topography statistics) were selected using an initial threshold, $\alpha_{cluster}$, and significant differences between conditions were then obtained by comparing the cluster T-values with a null distribution obtained using the Monte Carlo method. These Monte Carlo simulations were always computed using 1000 randomizations and an alpha value of 0.01 was considered for defining clusters and for the final hypothesis test. Differences between potentials recorded at the two stable epochs of perception were compared but considering only the potential across the entire time window for each condition (SB and SU). Finally, average asymmetry estimates using the AFA index value were compared between three separate windows, pre, post- and during a perceptual change, for both BU and UB epochs, using a 2-way ANOVA followed by post-hoc Tukey test, with correction for multiple comparisons.

3. Results and Discussion

In this section of the work, all results obtained and discussed will be presented. First, the results regarding the dynamics of event-related potentials driven by perceptual switches will be presented and how these are related to the data presented in Costa et al. (2017). Afterwards, an assessment of the hypothesis linking asymmetric oscillatory activity of the EEG signal and the slow components observed in ERPs was carried out.

3.1. Stimulus Perception

The stimulus presented to naive subjects to study mechanisms of visual organisation and perceptual binding consisted of a symmetric striped pattern, with angled black lines over a white background, forming a figure resembling a "roof" pattern (Figure 3.1). The lines described a continuous movement which for each half of the symmetrical image is ambiguous given the issues related to the aperture problem and the impossibility of defining the true physical motion of one-dimensional elements seen through an aperture, in this case a rectangular window. During the entire experiment participants maintained central fixation of gaze in a blue cross present during baseline and stimulation. In this viewing setup, the stimulus could be perceived in two configurations, which would alternate in a typical bistable behaviour. A Bound configuration where the moving lines on both sides of the stimulus appear as one and line up on the same central axis. It presents itself with a downward movement (Figure 3.1A). An Unbound configuration, where the lines on both sides appear offset and disconnected, like two independent images with an inward movement (Figure 3.1B).

This stimulus presented in Figure 3.1 is based on the work of Wallach (1935) (Wuerger, Shapley and Rubin, 1996) and recalls the typical illusion of barber poles, where ambiguous motion is determined by the aperture's shape. This stimulus is a combination of two symmetrical patterns in order to present two different images in each visual hemisphere that due to its inherent ambiguity can be perceived as either describing the same direction of motion or opposing ones. Subjects pressed and held

a specific button for each type of configuration they perceived at the time of observation.

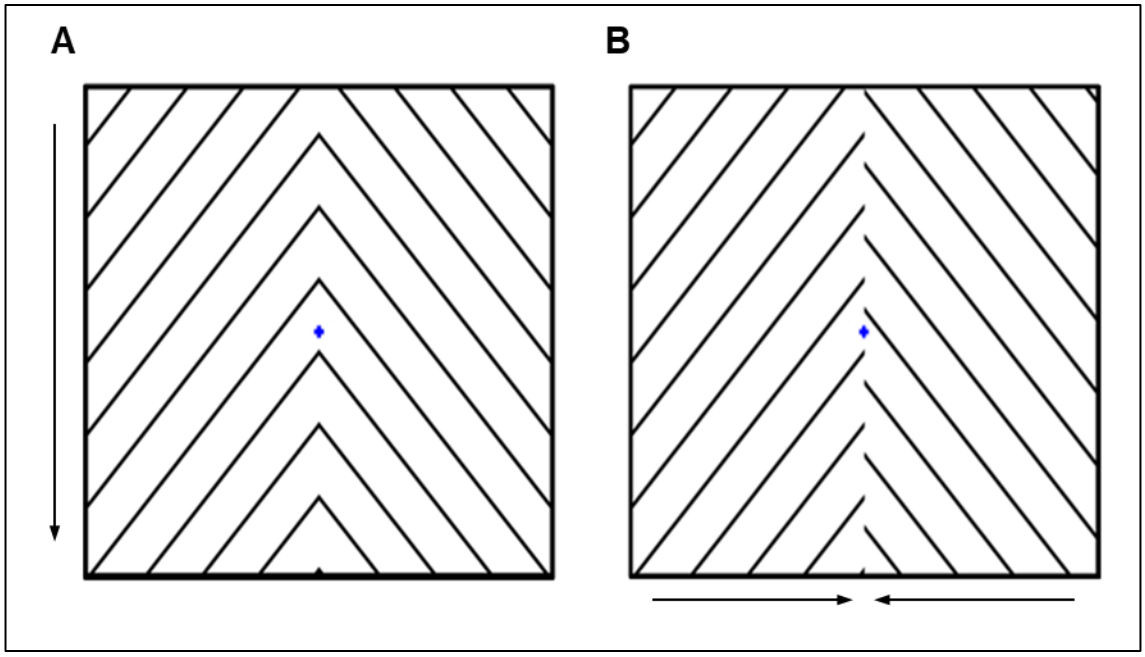

Figure 3.1. Ambiguous moving stimulus based on Wallach (1935). (**A**) Depiction of the Bound configuration, where both sides of the image are perceived as following the same vertical path, in perfect alignment (i.e., the lines meet at the center with no lag). (**B**) Representation of the Unbound configuration, characterized by horizontal motion towards the center and an illusory border separating both sides, which can also appear out of phase. A blue fixation cross was present during the entire stimulus duration. Arrows in A) and B) indicate the perceived direction of motion.

3.2. EEG Data and Oscillations for Perceptual Changes

In this section, the epochs that represented moments of perceptual switch were analysed. These epochs correspond to switches from a Bound to an Unbound perception and Unbound to Bound perception, referred from here on as BU and UB respectively. Assessments were made to the potential differences of the two configurations for the same latency period or for periods before and after the perceptual change. The average reference is the norm in EEG studies and is also the most accepted by researchers, however, a different analysis is performed using the Surface Laplacian/CSD reference-free method so that the results are not influenced by the reference choice.

3.2.1. ERP Analysis using Average Reference

It is known that the reference selection is a key factor, because each EEG electrode only informs about the difference in electrical activity between two established positions on the scalp (Lei and Liao, 2017). Knowing that the average reference is one of the most consensual and used references, is based on a conception that all potentials along the surface of the scalp are equal to zero, and that this approximation becomes more valid with a dense scalp sampling -greater number of channels leads to greater coverage of the total scalp surface and a more accurate spatial sampling (Junghöfer et al., 1999)- this was used as the first option for data analysis.

The epochs representing perceptual changes, BU and UB, were filtered with a 30 Hz lowpass filter. Frequencies above 30Hz typically don't produce measurable effects in terms of event-related potential (Luck, 2014). Together with previous findings using the current bistable figure and other bistable paradigms (Engel, Fries and Singer, 2001; VanRullen, 2006; Piantoni et al., 2017) showing most effects to arise from alpha and beta, activity in the gamma frequencies were not studied here. An ERP was established for each channel and averaged across subjects in the experiment.

Then, to assess the significant differences in the ERPs for the two perceptual changes, a statistical test was performed, a cluster-based statistics test with Monte Carlo permutations between the two conditions BU and UB for the whole time window (α_{clust} <0.01, for cluster-maximum statistics, and α_{stat} <0.01, for the null distribution obtained with Monte Carlo simulations, 1000 permutations). Statistically significant differences are displayed in Figure 3.2 (gray mask) overlaying the mean ERPs for each perceptual condition.

It is possible to observe in Figure 3.2 that parietal and occipital channels are the ones with the largest activation and with several clusters of contiguous statistically significant potentials. Nonetheless, this analysis also shows significant differences in more frontal electrodes, namely on the left and right sides of the scalp. On the other hand, central, temporal and temporal-parietal electrodes there is almost no statistically significant difference, which leads to believe that the overall activity related to perceptual changes is concentrated in displaying an apparent anti-correlated activity: posterior areas show a highly positive potential for changes to bound (post-change period of UB epochs) and a negative potential for unbound (post-change period of BU epochs), while frontal areas show the opposite pattern. It is also possible to observe that the channels that display statistically significant differences, the great majority have it after the perceptual report through button-press, that is, the great change in potentials happens, in general, a few msec after the subject's perceptual change.

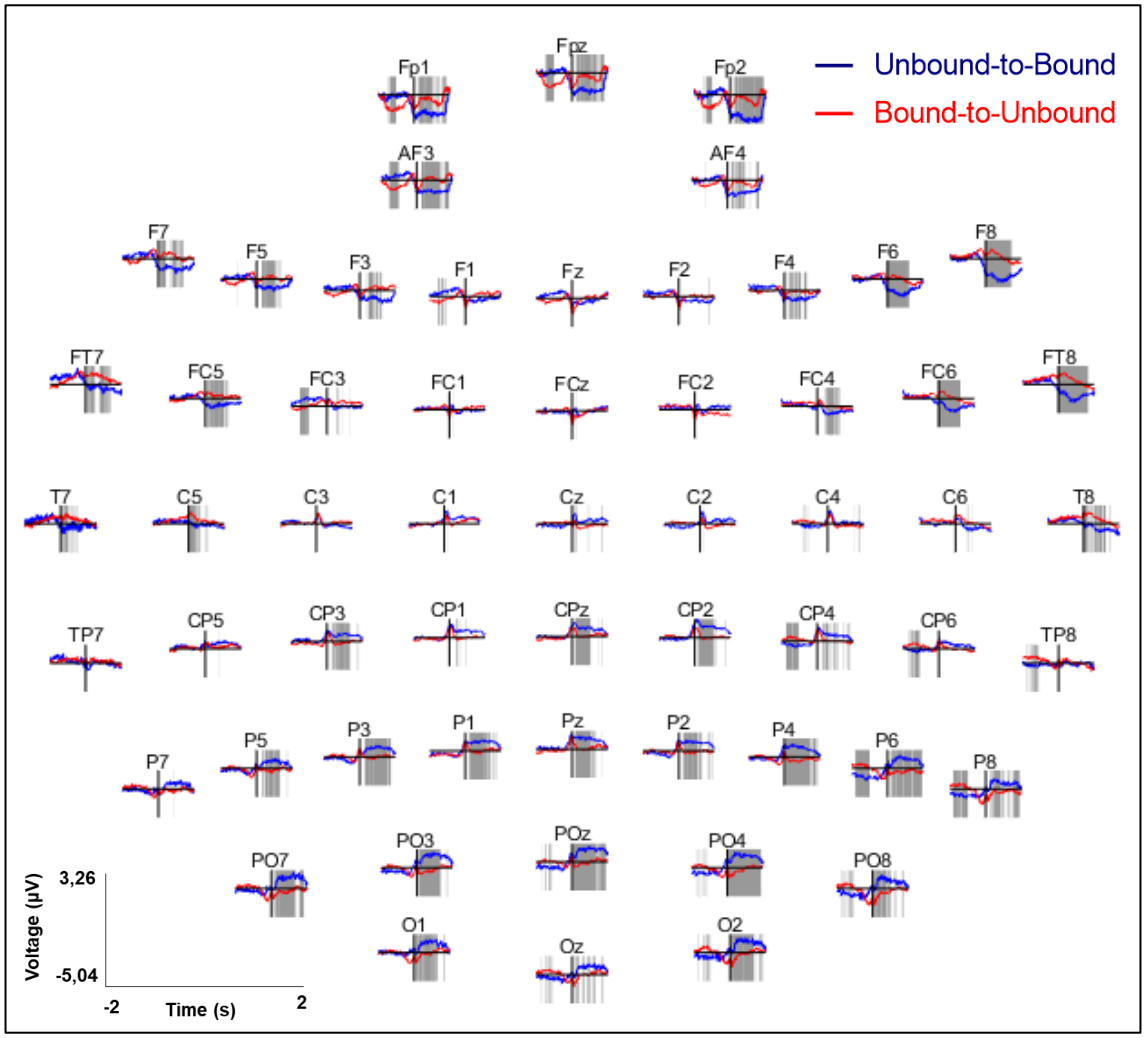

Figure 3.2. Topographic Representation of mean ERP of all subjects for Periods of Perceptual Transition throughout all scalp electrodes (Average Reference). Corresponding channel labels depicted above each ERP. Perceptual changes from UB (blue) and BU (red) are represented in the same plots for each channel, highlighting differences between conditions in several channels. ERPs estimated on time-locked windows consisting of -2000 msec to 2000 msec for average referenced EEG. The zero msec line represents the moment of perceptual report. Significant areas are shown in grey (cluster-based statistics with Monte Carlo permutations, $p < 0.01$).

The change from UB configuration is the one that presents the greatest amplitude of ERPs over the defined temporal window. In the frontal electrodes there is a shift towards negative potentials for periods that follow the perceptual change. In the frontal channels found in the left and right hemispheres, these variations are even more evident, as is the case of electrode F8, where it is possible to observe that before the instant 0 sec, the potential has low amplitude and modulation and then suffers a great reduction, starting to present amplitudes of up to -5 μV. As for parietal and occipital electrodes, the voltage values of the potentials are at a baseline level pre-change periods, but for the post-change periods this time they present positive voltage values. For example, on electrodes PO7, O1, P4, POz and O2, it is possible to clearly observe this increase in potential amplitude, but for positive voltage values when there is a transition to the Bound perception configuration, inversely to what happens in frontal electrodes. Some of these mentioned as an example, have amplitudes in the order of 3 μV.

Regarding the ERPs representing BU epochs (displayed as red traces in Figure 3.2), it is observed that in periods prior to the perceptual change there are reductions in the frontal electrodes. These modulations are more evident in those located in the most anterior part of the head, as is the case with FP1, FPz, FP2, with amplitudes of around -2.5 μV. In the frontotemporal and temporal channels there is a small increase in ERPs, but with low amplitude. In the parietal and occipital electrodes, the potential remains stable but with a small reduction close to the response-related trigger and with amplitudes of -1 μV. Related to the period following the perceptual change, the ERP shows very little variation in almost all channels, with the exception of small increases in the posterior and anterior part of the scalp (O2, O1, PO8, FP2, FPz, FP1) and small reductions in the channels of the left and right hemispheres (FT8, F8, F6, F7, FT7).

These findings can correspond to either two anti-correlated sources, in diametrically opposed cortical regions, that activate during perceptual change and perceptual report events, or by a single dipolar source centered close to the vertex electrode (Cz) and tangentially oriented towards the front of the scalp along an posterior-anterior axis. This could also be a result of the reference method of choice, namely the average reference, which assumes the average potential of the scalp as zero and can

inadvertently create distributions of potential that are consistent with dipolar sources but do not represent the actual cortical activity. This can be explained by the polar average reference effect described in Junghöfer et al. (1999), which states that this bias caused by the average reference affects the potential amplitudes to be smaller in the electrodes that are in the centre of electrode array than on those found in more peripheral areas.

In a general analysis of the central electrodes, it is possible to observe that for the two configurations the mean ERPs present the same behaviour: Variation almost null before and after the perceptual change, with amplitude peaks up to 2 μV around the instant 0 sec. This type of experiment requires a response from the volunteers to indicate the moment in which the perceptual transition occurred, and this signalling is done through a button-press. It is also known that button-pressing produces potential motors in the central region of the brain, therefore affects mostly central electrodes but also affects the latency and amplitude of other ERPs (Salisbury et al., 2001). However, in an attempt to minimize these so-called effects, the experiment was carried out with the right hand in one half and the left hand in the other half, but the motor response is still identifiable as in electrodes C3, C1, Cz, C2 and C4.

Nonetheless, the potentials that are significant and relevant do not come from the motor response. no-report bistable perception studies have been devised for particular paradigms for which perception can be tracked through eye movements for instance (Tsuchiya et al., 2015), but no such reliable signal was likely to result from the current paradigm. Using constant dual motor reports and interpreting potentials far from motor and somatosensory cortical areas an attempt was made to minimize the effects of motor responses.

As can be seen in Figure 3.2, the most statistically significant channels are the occipital and parietal channels on the right side of the scalp. Consequently, it was decided to present an average ERP of these channels, respectively P2, P4, P6, P8, PO4, PO8 and O2. It was plotted with a time window of -2 to 2 sec, where 0 represents the response-related trigger and the ordinate axis represents voltage values in μV (Figure 3.3A). This mean ERP is shown in Figure 3.3A, with a time window of 2000 msec before and after the reported perceptual switch, signalled at 0 msec.

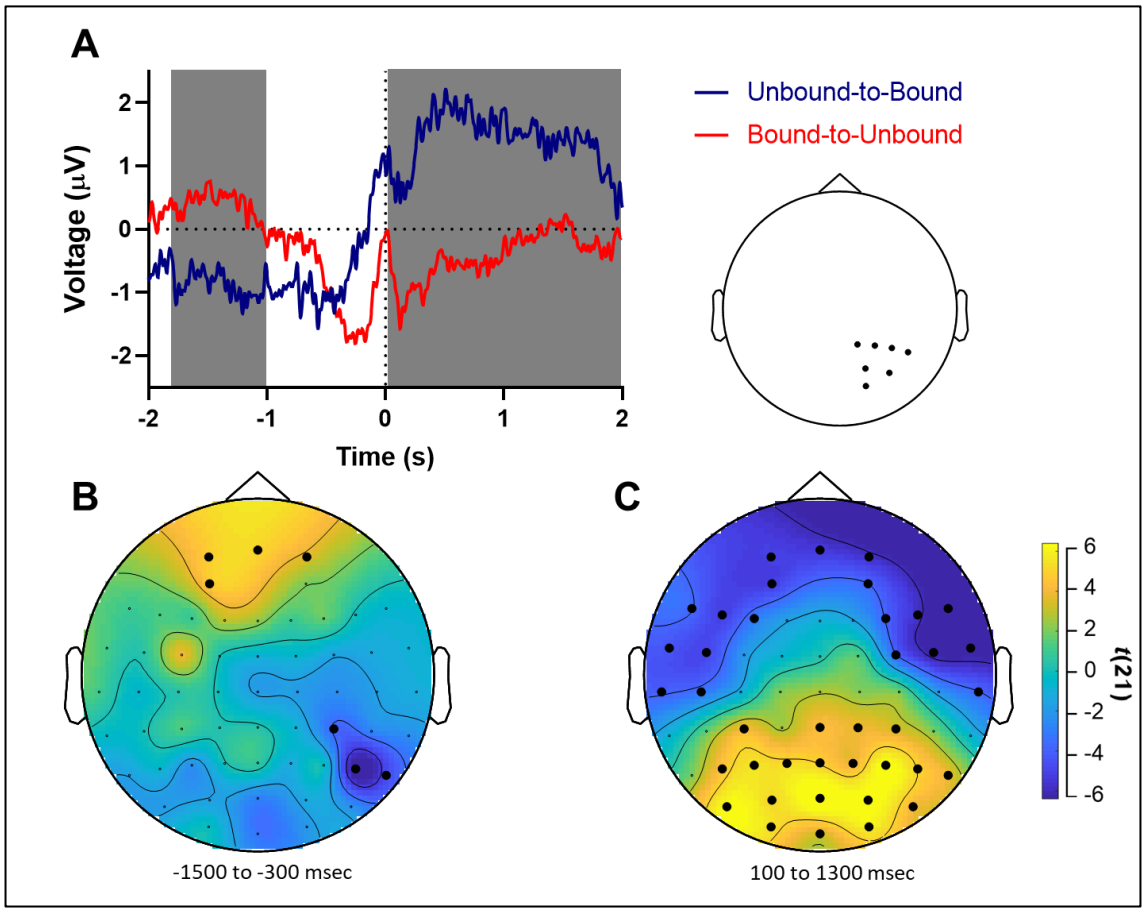

Figure 3.3. ERP for Selected Channels and Significant Ones for Different Periods of Time throughout Perception (Average Reference). (**A**) Event Related Potential for Periods with a Perceptual Transition of channels P2, P4, P6, P8, PO4, PO8, O2 using average reference. Significant areas in grey (cluster-based statistics with Monte Carlo permutations, $p < 0.01$); The zero in the x-axis represents the moment of perceptual report. The locations of channels represented in the ERP are displayed in the topography at the right. (**B**) Topographic distribution of T-values achieved with statistical test between epochs with a Perceptual Transition with an average reference for period of interest of -1500 msec to -300 msec, with significant channels marked with black dots (cluster-based statistics with Monte Carlo permutations, $p < 0.01$). (**C**) Representation of T-Values similar to the topography in B but with a different time window, 100 msec to 1300 msec, also with the significant channels marked with black dots (cluster-based statistics with Monte Carlo permutations, $p < 0.01$).

The UB configuration starts with amplitude values around -1 μV. This amplitude is maintained from the beginning of ERP until about -300 msec. However, milliseconds before indicating the perceptual change, the potential is modulated and undergoes an increase, starting to have amplitude values that are around 1 μV and 2 μV. This amplitude is maintained until 2000 msec but with a gradual decrease, reaching an amplitude of 0.5 μV at 2000 msec. The BU configuration, on the other hand, starts with amplitudes of 0.5 μV between -2000 msec and -1000 msec. Then the potential decreases, even reaching an amplitude of about -2 μV. A peak is observed at time 0 msec, practically without amplitude, and then a new sudden decrease that is followed by a gradual increase. After the report, there is an average negative potential of -1 μV lasting for about 1000 msec. The parts of the ERP that are statistically significant are the regions where the difference in potentials between the two configurations is most pronounced, specifically, from -1800 until -1000 msec and from 0 until 2000 msec.

The increase and the peak observed in the two potentials at 0 msec is due to the motor response that the participants of the experiment made when they pressed the button to signal the perceptual change. This ERP is similar between both conditions and is embedded in a larger potentials that shows a similar dynamics as the power spectrum of beta waves during perceptual change (see Figure 3.6 and discussion below)

As differences between the two conditions occur during periods corresponding to both before and after the perceptual transition, two periods were defined to evaluate the topographical distribution of these differences. The pre-change period was set from -1500 until -300 msec and the post-change period from 100 until 1300 msec, with both periods consisting of 1200 msec. Two statistical tests were carried out in the FieldTrip toolbox between the BU and UB epochs. Both are cluster-based statistics with Monte Carlo permutations (1000 randomizations; alpha value of 0.01). The T-values resulting from the statistical test for the pre-change period are shown in Figure 3B. For the post-change period, the T-Values are represented in Figure 3C. Results were plotted on scalp topographies with statistically relevant channels represented with black dots.

During the period preceding the perceptual transition, it is seen that there are frontal channels with positive T-Values, that is, positive values means that the UB condition

has a bigger potential than BU. Electrodes FP1, FPz, FP2 and AF3 are the ones presenting significant differences. At the posterior part of the head, in the right hemisphere, we have channels such as CP4, P6 and P8 that present negative and relevant T-Values, with UB condition having lower potential than BU. This reveals that there is a difference between the anterior and posterior regions of the scalp and resembles an electric dipole, because the rest of the scalp presents T-Values near 0 and the potentials of each configuration are inverted with respect to each other. Looking at the topography for the period after the perceptual switch, differences are even more evident than in the pre-change period. Differences are once again seen in anterior and posterior areas, with central channels displaying no significant differences between conditions. The topography shows a clear negative difference for frontal potentials, meaning that BU configuration has a bigger potential, while more posterior areas show a positive difference, also meaning that the UB configuration is the one with bigger voltage values. This results from the higher positive potential before a perceptual change from BU when compared to a change from UB, which after the perceptual change displays the opposite pattern. These pre and post-perceptual change potentials then lead to topographies with an inverted pattern, as seen in Figure 3.3B.

3.2.2. ERP Analysis using Reference-Free Method

For reasons that were previously discussed, the reference-problem in EEG and thus the selected reference used to analyse data was taken into account in this study. The data and ERPs were analysed using average reference, which while fairly reliable and relatively unbiased, carries several assumptions regarding the origin and the distribution of neuroelectric potentials in the scalp. In an attempt to clarify the nature of the perceptually driven potentials, we performed a similar analysis using a reference-free method. As the differences observed suggested a modulation of brain activity that results in potentials with opposing signs between anterior and posterior regions, this could also be an artifact of the selected reference method that assumes a net charge of zero for the entire scalp. Thus, we re-referenced the ERPs to the Surface Laplacian/CSD method, which provides higher spatial resolution to the recorded signal and higher topographic specificity. A spherical spline computation method was used to re-reference the perceptual change epochs, i.e., BU and UB epochs.

Then, statistical tests similar to those computed to the data referenced by the average (cluster-based statistical test with Monte Carlo permutations) were performed. The alpha value is 0.01 and the statistical time window is the same as the epochs' duration. Significant differences between the Surface Laplacian-referenced BU and UB epochs are highlighted in gray in Figure 3.4, where the ERPs of all channels are represented. The significance is once again determined by a permutation test with control for multiple comparisons.

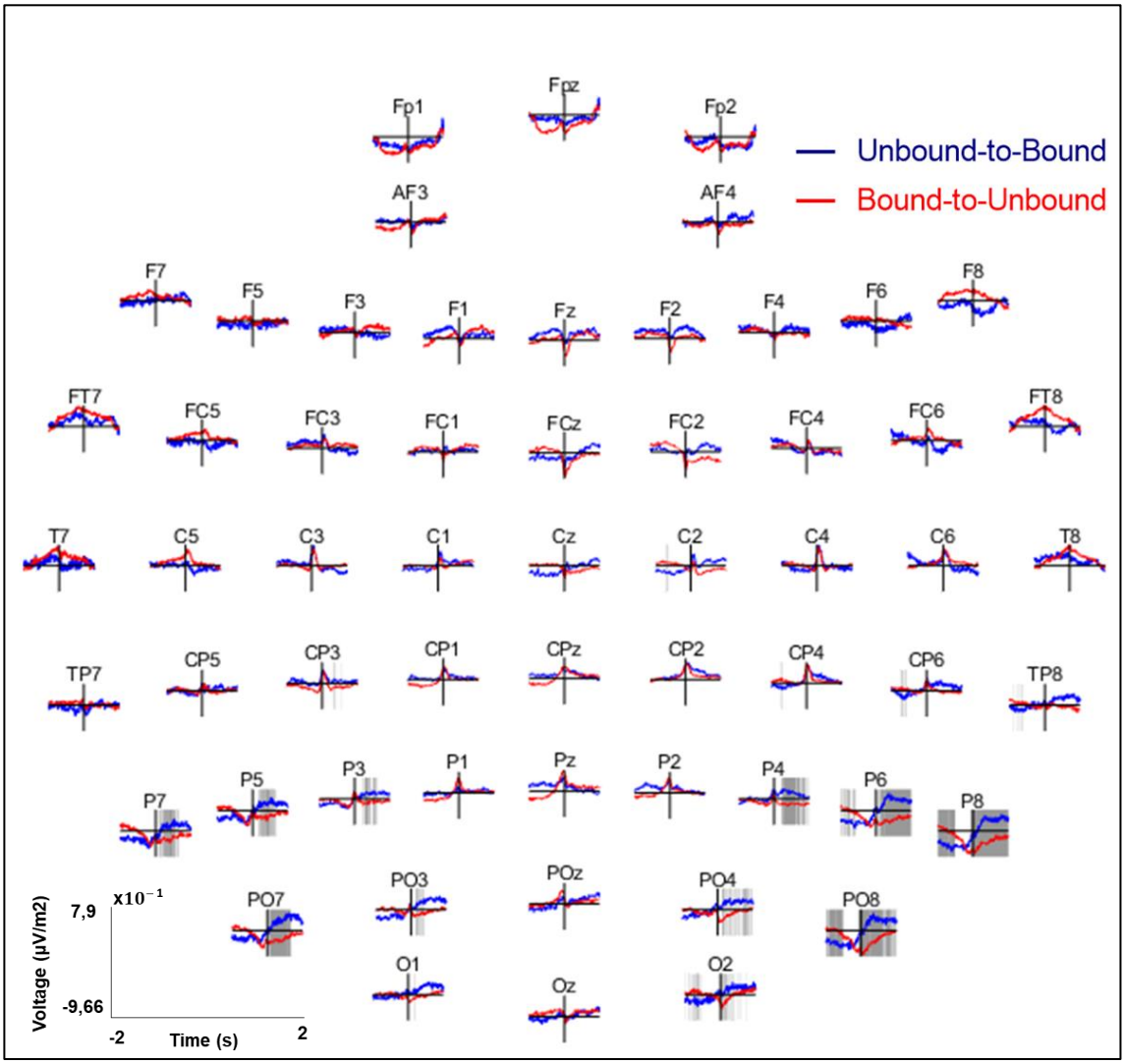

Figure 3.4. Topographic Representation of mean ERP of all subjects for Periods of Perceptual Transition throughout all scalp electrodes (Reference-Free). ERPs depicted as in Figure 3.2, with the correspondent label above each channel, estimated using the reference-free method Surface Laplacian/CSD. Differences between conditions appear in a more restricted set of scalp electrodes, compared to Average referenced ERPs in Figure 3.2. The time window for each electrode is from -2000 msec to 2000 msec; The zero represents the moment of perceptual change; Significant areas in grey (cluster-based statistics with Monte Carlo permutations, $p < 0.01$).

The electrodes with statistically significant differences are only located in the posterior region of the scalp, namely those located on the right and left side of the head. Significant differences are found parietal (P7, P5, P3, P4, P6, P8), parieto-occipital (PO7, PO3, PO4, PO8) and occipital channels (O2). Compared to Figure 3.2, it can be seen that the reference-free data is much more specific in spatial terms and that the difference between the two conditions only occurs in specific sets of channels. It is also observed that in both figures, the largest differences occur in periods of time after the perceptual change. In the electrodes on the back of the head, for the UB condition, the voltage is negative before the perceptual change and then rises and reaches positive values after the change, while for the BU condition the opposite happens. This phenomenon is in accordance with what Figure 3.2 shows for the same electrodes, i.e., it is independent of the type of reference.

In agreement with the observations for the data with average reference, certain electrodes in the occipital and parietal area on the right hemisphere displayed more evident differences within the ERP timecourse. The average ERP of these electrodes is shown in Figure 3.5A. The presented ERP is very similar to the one in Figure 3.3A, as it also presents negative amplitude values for pre-change periods in the UB configuration, followed by a peak close to 0 msec and a continuous rise that ends up plateauing at positive values, around 3 μV/ m2 of amplitude, for a post-change period. Scalp potentials for the BU perceptual change starts with a slight decrease, followed by a small peak at 0 msec and then a small increase but always with negative amplitude values. As previously mentioned, these peaks observed at 0 msec in both conditions and in both ERPs (Figure 3.3A and Figure 3.5A), are due to the motor response responsible for the push of a button to signal the perceptual switch. This average ERP is also very similar to the power spectrum of beta waves of EEG signal, as the previous average-referenced ERP. This reveals that the reference has little influence on the overall shape of the ERPs presented but supports the hypothesis that it has a great influence in the spatial specificity with which the data can be evaluated, since the reference-free method allows for a clearer notion of potentials' location that are directly related to the task performed by the subjects. Further confirmation of these potentials' sources can be achieved with adequate source localization methods, such

as beamforming spatial filters in the time-domain (.e.g linearly constrained minimal variance, or lcmv, beamforming).

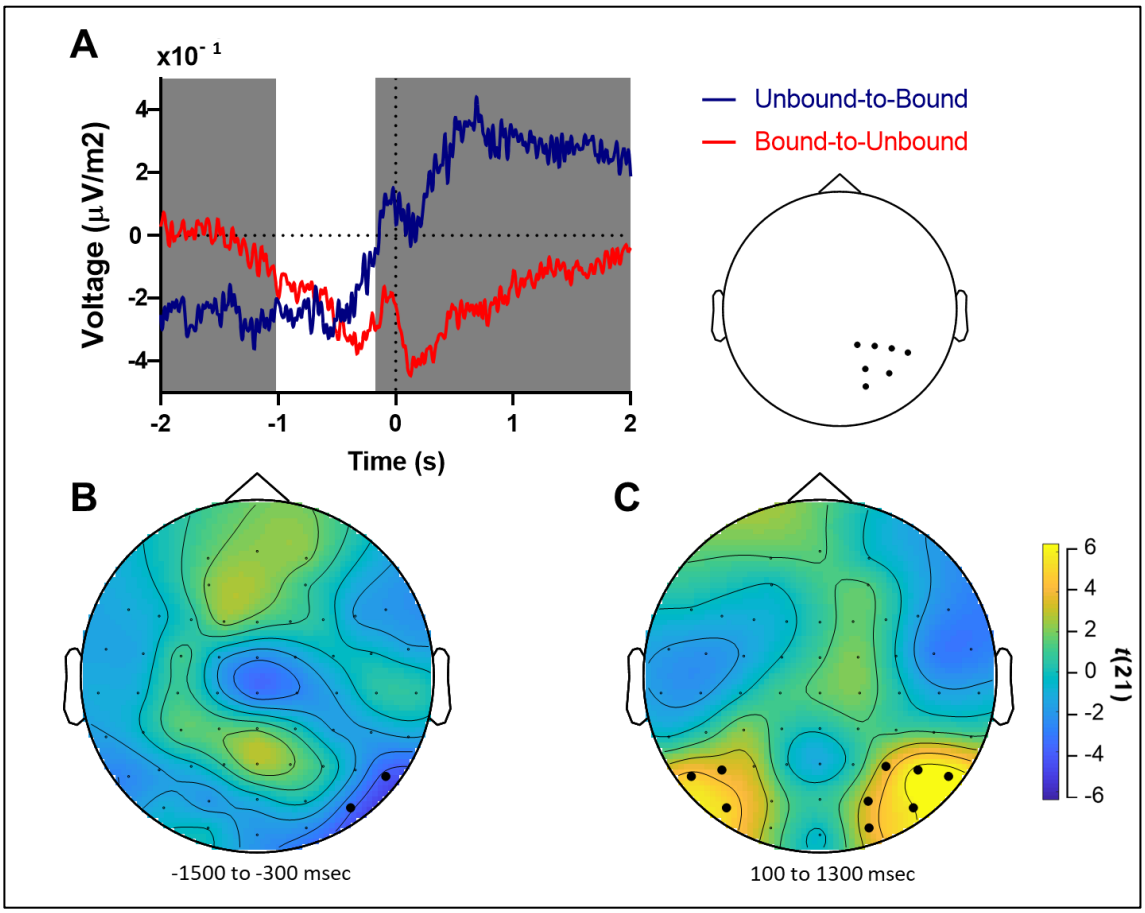

Figure 3.5. ERP for Selected Channels and Significant Ones for Different Periods of Time throughout Perception (Reference-Free). (**A**) Event Related Potential for Periods with a Perceptual Transition of channels P2, P4, P6, P8, PO4, PO8, O2 using reference-free method Surface Laplacian/CSD. Significant areas in grey (cluster-based statistics with Monte Carlo permutations, $p < 0.01$); The zero in the x-axis represents the moment of perceptual report. The locations of channels represented in the ERP are displayed in the topography at the right. (**B**) Topographic distribution of T-values achieved with statistical test between epochs with a Perceptual Transition with a reference free for period of interest of -1500 msec to -300 msec, with significant channels marked with black dots (cluster-based statistics with Monte Carlo permutations, $p < 0.01$). (**C**) Representation of T-Values similar to the topography in B but with a different time window, 100 msec to 1300 msec, also with the significant channels marked with black dots (cluster-based statistics with Monte Carlo permutations, $p < 0.01$).

To evaluate the locations and differences between the two conditions in periods before and after the perceptual exchange, the same procedure was applied to the UB and BU epochs referenced with the CSD method as the ones computed with the average reference. Two statistical tests with different latency periods: a pre-change period (-1500 msec to -300 msec from the perceptual report) and a post-change period (100 msec to 1300 msec). Channels with statistical significance were marked with black dots.

For the pre-change period, the topography of potential differences between epochs consisting of changes to bound vs changes to unbound perception evidenced significant differences in the right parieto-occipital areas: over electrodes PO8 and P8 (Figure 3.5B). There is overall a more negative potential for the activity recorded pre-change to bound when compared to the pre-change to unbound. Compared to the differences in scalp potentials analysed with an average reference, shown in Figure 3.3B, it reveals that the differences are more localized in posterior areas, around the parietal and occipital areas and more evident on the right side of the scalp.

For the post-change period (100 msec to 1300 msec post-perceptual report), the difference in potential between the two conditions, BU and UB, show positive values on the posterior electrodes, mainly in two groups over the parieto-occipital areas: PO7, P7 and P5 on the left side and O2, PO4, PO8, P4, P6 and P8 on the right side. The t-values in the topography represent more positive potentials for the bound percept compared to the unbound percept. Making a comparison with the same comparison for the average-reference data, Figure 3.3C, there is a large difference in location of the observed differences and greater specificity in terms of significant channels. This makes perfect sense, after knowing that this new type of reference has a higher topographic specificity than the average reference.

3.3. Time Frequency Analysis for Brain Oscillations

A time frequency analysis was carried out to understand which frequencies had the highest incidence in the spectrum of the EEG data under study and whether the frequency bands chosen for the results make sense and are in accordance with the results shown in Costa et al., 2017. This time frequency analysis was performed for the BU and UB epochs with average reference. For this evaluation, the type of reference chosen does not affect the frequency analysis and spectrogram of induced responses (due to power being independent of the potential signals, whether positive or negative, and due to baseline normalization that result in relative changes) and for this reason it was made only for these epochs.

Using the FieldTrip toolbox, a power spectrum was obtained for each type of condition (BU and UB) and for each subject. Then, an average spectrogram was obtained for each condition (Figure 3.6A and 3.6B). They have been plotted with the total duration of the epoch, -2.5 until 2.5 sec, and the frequency range is from 8 to 60 Hz. The moment 0 sec represents the perceptual change of the subjects.

In Figure 3.6A, the spectrogram shows a clear zone of higher power. It is marked in red, with a positive power and after the moment 0 sec, which corresponds to the perceptual change reported by the subject. The most active frequency range is 13-20 Hz, that corresponds to beta waves, which appears with greater activity and incidence from 0 until 1.5 sec. It is also possible to observe that between 1.5 and 2.5 sec there is an increase in power but for frequencies that fall within the range of alpha waves. For Figure 3.6B, the incidence of power of EEG activity occurs between -1 and 1.5 sec, with negative power and in the frequency range of beta and alpha waves. There appears to be an even distribution but with slightly increased beta wave activity.

A time course analysis of oscillatory activity was also performed for the frequency range of beta waves (13-30 Hz), the range that has been studied throughout this work. Through averaging processes, an average absolute power of beta frequency bands was created, from the power spectrum of Figures 3.6A and 3.6B. The plot in question is represented in Figure 3.6C, and it was used a baseline from -1.5 until -1 sec for

visualization purposes. In this figure, the UB condition has larger power than the BU practically throughout the entire period following the perceptual change. For the period before the change, the BU condition has slightly more power, it has a small decrease right before 0 sec. Briefly, before the change, BU has superior power than UB, and after the change the roles are reversed.

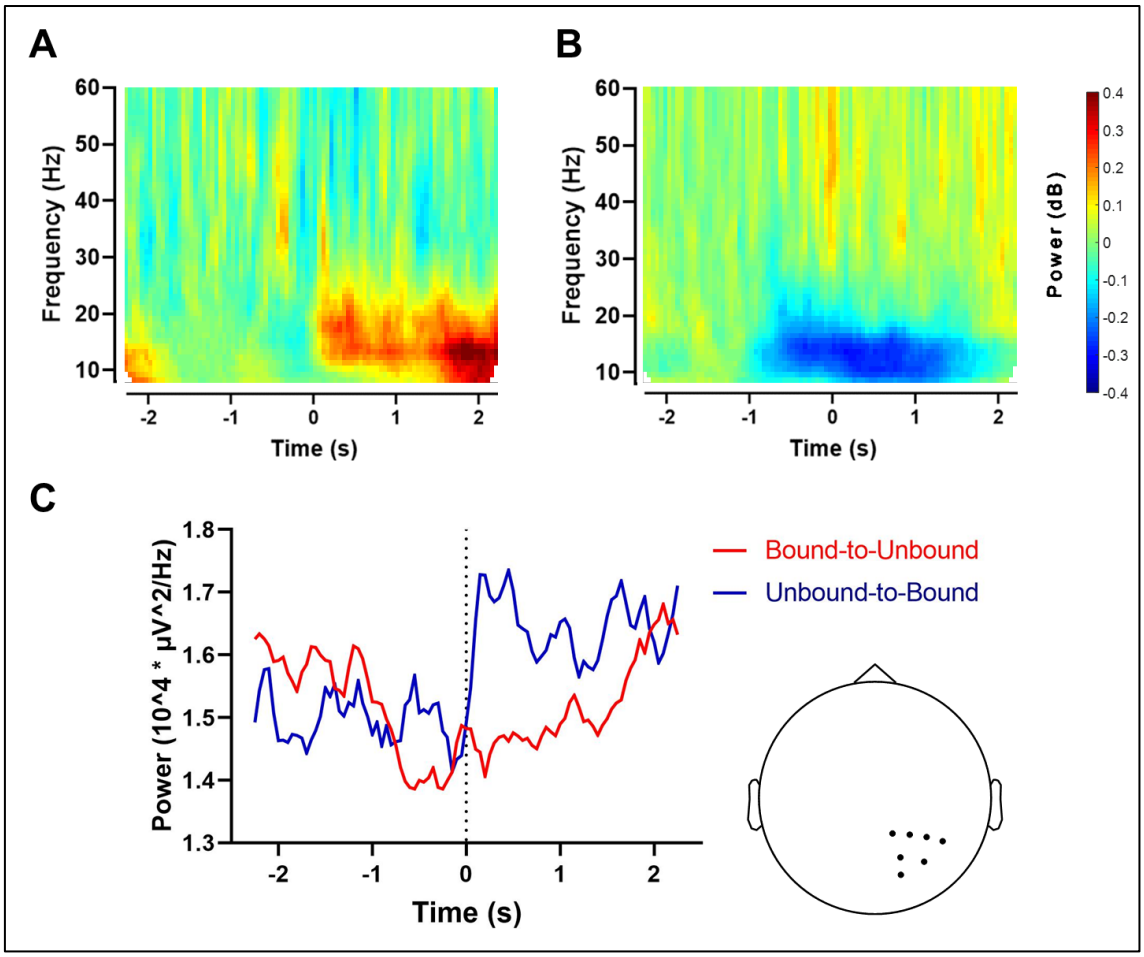

Figure 3.6. Time course of Brain Oscillations during Perceptual Changes. Spectrograms of transitions epochs from UB perception (**A**) and from BU perception (**B**). The zero-time point represents the moment participants reported the switch. The interval from −1.5 to −1 sec was used as baseline for visualization purposes. (**C**) Time course of average absolute power for beta frequency band and for selected channels, represented in auxiliary topography on the right.

It should be noted that Figure 3.6C only represents the average power for the beta frequency band and for the channels selected throughout this study. They are the occipitals and parietal's ones on the right side of the head and are represented topographically in the inset. However, the figure representing the time course of beta waves in Costa et al., 2017 represents the average power for the same frequency band, but for all head electrodes. Nonetheless, these beta differences during perceptual change and also during stable percepts are more evident in occipital and right parietal areas.

Making a comparison with the average ERPs of the selected channels shown in Figures 3.3A and 3.5A, we realize that there are some interesting aspects that can be the subject of comparisons and discussions. Figures 3.3A and 3.5A reveal that, regardless of the reference that was used, the potentials are similar and that the variations over time are the same. In both figures, we see that the UB condition starts before the perceptual switch with negative potentials. In the topographies (Figures 3.3B and 3.5B) the differences between the potentials for this latency period indicate that the UB potentials are smaller than the BU condition, and this is visible in Figures 3.3A and 3.5A. Following the perceptual switch, the potentials suffer a modulation: UB has a large increase and then stabilizes, BU has an immediate decrease after the switch and then a slight rise but always with negative amplitudes. In the differences of potentials, we see that for the moment following the exchange, an inversion takes place. UB potentials become larger than BU potentials.

These slow variations that are observed in Figures 3.3A and 3.5A are also contemplated in Figure 3.6C, where there is, before the switch, a lower power for the UB configuration which is followed by an increase just after 0 sec and then it is maintained with some variations, and for the BU configuration with a higher power but with a decrease milliseconds before switching that follow a gradual increase up to 2 sec. This variation pattern is the same as those registered in ERPs and also the one registered in the time course of beta waves in Costa et al., 2017. This suggests that right after the switch to Bound perception, there is greater activation of beta with higher concentration in the occipital and parietal electrodes. This phenomenon is accompanied by an increase in the positive amplitude of the potentials captured on

the scalp for these same electrodes. However, when the subject passes from a Bound to an Unbound perception, there is less activation of the beta milliseconds before signalling the perceptual change, which also culminates in potentials with more negative amplitudes.

3.4. Evaluating the Impact of Amplitude Fluctuation Asymmetry in Brain Oscillations

Because the modulations and variations of the ERPs that we observe in Figures 3.3A and 3.5A have a duration of several hundred milliseconds, these can be considered as slow components of the overall ERP. These slow changes in potential follow a similar timing as the previously measured changes in beta activity (Costa et al 2017). A model proposed by Mazaheri and Jensen, 2008 offers a possible cause for these co-occuring differences in both ERPs and in spectral changes: when an EEG signal has an amplitude asymmetry, either with a depression or an increase in oscillatory activity in response to the stimulus, a slow component is created after an event-related averaging process. This model can help us understand how a change in beta oscillations might be associated with a slow change in scalp potentials. This is observed in Costa et. al. 2017 and in Figure 3.6, when the power time course of beta waves in epochs with perceptual change has an increase in the change to-bound configuration and a decrease in the change to-unbound configuration. These modulations are also perceptible in ERPs from the same epochs that involve perceptual changes. Mazaheri and Jensen, 2008 proposes that these slow variations that are observed in the ERP are related to the asymmetry present in the oscillatory activity of the EEG. The proposed hypothesis is that the asymmetry in the oscillations measured in the EEG is the cause of the slow ERP components and is associated with changes in the power time course of the beta oscillations. Based on this hypothesis, it was decided to evaluate whether the slow components observed in the ERPs are related to the asymmetry of the oscillatory activity measured in the EEG.

To quantify the amplitude asymmetry, we adapted the formula used in Mazaheri and Jensen, 2008, which is called the AFA_{index}. AFA stands for Amplitude Fluctuation Asymmetry and measures the variance of peaks and troughs of EEG signal activity (Figure 3.7D). For a better understanding of the application of the formula, see the Asymmetry Analysis Section in the Methods Chapter.

In order to test this AFA_{index} and verify if it was a good indicator of the asymmetric modulation for the amplitude of EEG waves, it was decided to simulate data computed with an asymmetric configuration. The wave function used to simulate was $A(t) \cdot (1 + \sin(2\pi f t + \varphi)$, where $A(t)$ is a sigmoid function: $A(t) = a - \frac{b}{1+e^{t/0.2}}$ and for these simulations it can take two forms: a depression or an increase over time (Figure 3.7C). The variable f represents frequency and, in this simulation, takes the value of 10 Hz. One hundred trials were simulated for each amplitude function, in which each trial had the addition of white noise and a random phase φ. The time window used was from -2 until 2 sec and 0 sec represent the midpoint of amplitude function.

The simulated data were filtered with a 8-12 Hz bandpass filter to obtain peaks and troughs timepoints and applied them to the unfiltered data in order to calculate the AFA_{index}.

For each trial, an AFA_{index} value was calculated and an average of the 100 trials was performed, thus obtaining only one value for each type of amplitude function. Figure 3.7A demonstrates the first trial of the simulated data with a decreasing amplitude modulation, followed by the mean AFA_{index} value (0,8823). In Figure 3.7B, is a similar representation but with an increasing modulation and also accompanied by the respective average AFA_{index} (0.8822). Since the AFA_{index} assumes values between 0 and 1, where 0 represents no asymmetry and 1 total asymmetry, these values presented for the two figures reveal that the AFA_{index} is a suitable indicator to evaluate the asymmetric fluctuation of the amplitude of electrical activity of the scalp. However large the asymmetry used in these simulations, these values do not reach a value of 1 since all the trials had added white noise and a random phase in each one of them, which lowers the level of asymmetry established only by the wave function.

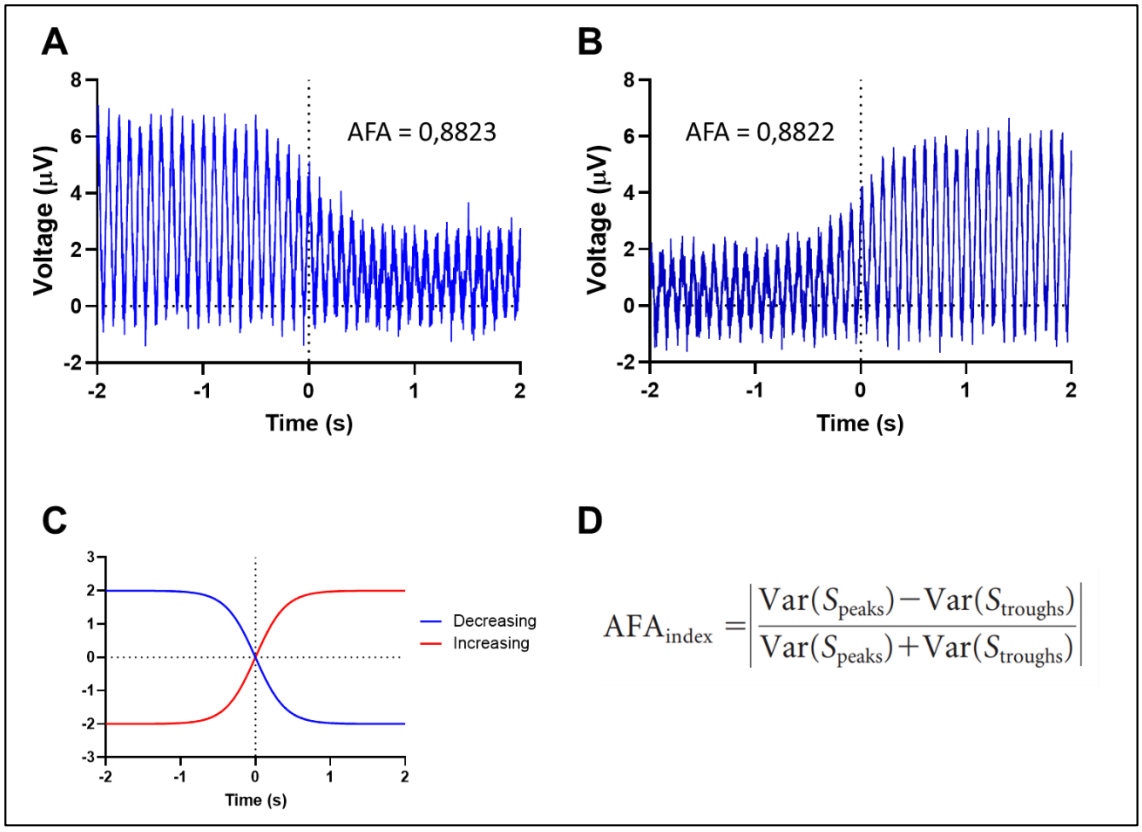

Figure 3.7. AFA_{index} Computations on Simulated Data. (**A**) First Trial of Simulated Data using a Decreasing Amplitude Function. This signal was created with an asymmetric wave equation $A(t) \cdot (1 + \sin(2\pi f t + \varphi))$ + white noise (f = 10 Hz). AFA_{index} of all 100 trials is 0,8823. (**B**) First Trial of Simulated Data using an Increasing Amplitude Function. This signal was simulated like the one in A, but with a different $A(t)$. AFA_{index} of all 100 trial is 0,8822. (**C**) Representation of the Amplitude Functions used in A and B throughout the time course. (**D**) Mathematical Formula used to compute the AFA_{index}. Adapted from Mazaheri and Jensen (2008) and only calculate absolute values.

3.5. Evaluating the Amplitude Fluctuation Asymmetry in EEG Oscillations in Empirical Data

After concluding that the AFA_{index} was a good measure to evaluate the asymmetry of the waves present in the oscillatory activity of the EEG signal, the index was applied to the empirical data, respectively to BU and UB epochs referenced by the Reference-free method Surface Laplacian/ CSD, to try to understand if the asymmetric modulation of the signal was behind the slow components observed in the previously described ERPs.

Epochs were bandpass filtered from 13-30 Hz, the frequency band of beta waves. This range was chosen because the slow components of the ERPs were also observed in the time course of the average absolute power of the beta waves of the EEG data.

The same method of calculating the AFA_{index} in the simulated data was used: Timepoints of peaks and troughs of the filtered data are applied to the previous data that had not been bandpass filtered to obtain the respective values of peaks and troughs and compute the AFA_{index}. The time window used for the calculation was from -2 until 2 sec. For each trial of each subject and each channel, we obtained an AFA_{index} value. After averaging across trials, there was now only one value for each electrode and for each subject. Another averaging occurred, but this time across subjects. The distribution of index values along the channels is displayed in Figure 3.8A.

For the BU configuration, Figure 3.8A reveals that the AFA_{index} remains practically at very low values, always oscillating between 0 and 0.1 Although there are some subjects who present higher asymmetry values for certain channels, around 0.3 between electrodes C2 and CP2, the vast majority are all index values close to 0, which demonstrate that the BU epochs are not asymmetric. As for the UB epochs, Figure 3.8A also presents results similar to those in the BU configuration. The vast majority of subjects, in virtually all channels, have AFA_{index} values close to 0, revealing that these epochs are not asymmetric either.

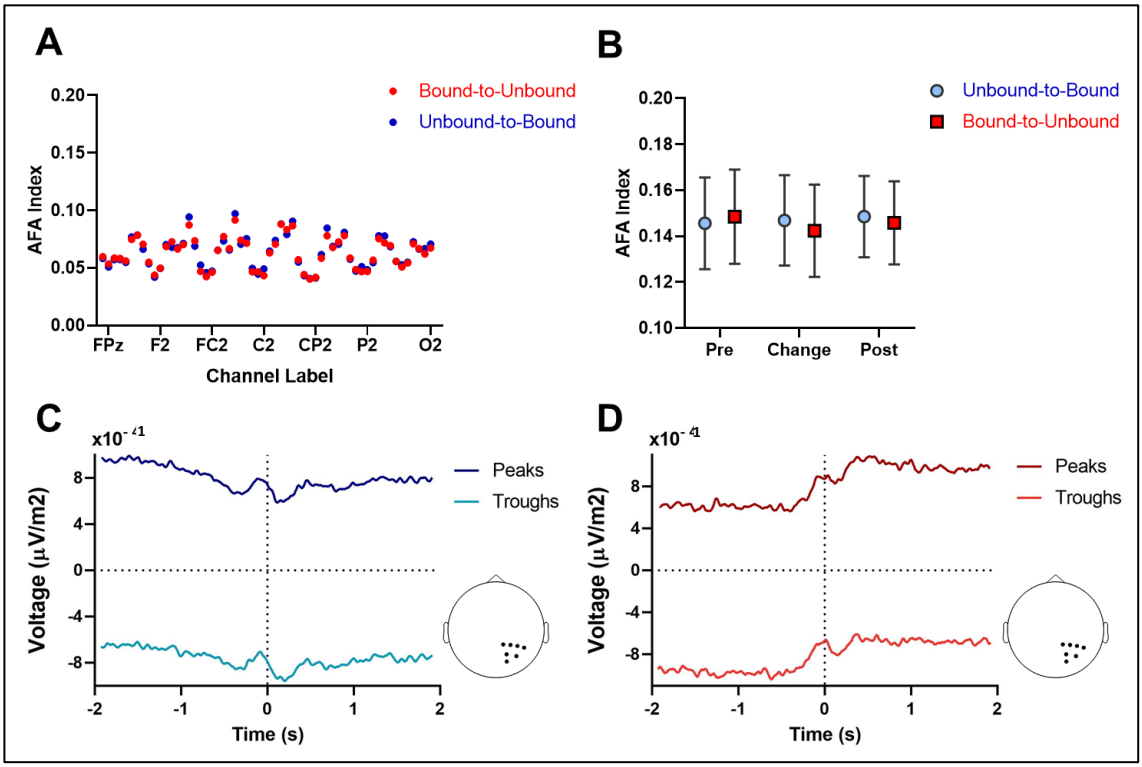

Figure 3.8. AFA_{index} Computations on Empirical Data. (**A**) Distribution of mean AFA_{index} of all 21 subjects throughout all channels for BU and UB conditions using the reference-free method Surface Laplacian/CSD. The data was band filtered 13-30 Hz (alpha waves frequency range) before the calculus. (**B**) Mean AFA_{index} values averaged across trials, subjects and channels plotted with respective Standard Deviations (Mean ± SD) for different periods of time in epochs (Pre: -2 to -1 sec; Change: -0.5 to 0.5 sec; Post: 1 to 2 sec) (**C**) Representation of time course of average voltage values for Peaks and Troughs in BU epochs. Auxiliary Topographic shows the channels chosen to elaborate the averaging process. (**D**) Similar Representation of average voltage values for Peaks and Troughs as represented in C but for a different configuration, BU. Auxiliary Topographic shows the channels chosen to elaborate the averaging process.

Assessing differences in AFA_{index} between periods of perceptual change vs reference periods of stable perception (pre and post-change) revealed a small effect of the time window (Two-way ANOVA, main effect time F (2, 40) = 3,384, p=0,0439; main-effect percept F (1, 20) = 2,494, p=0,130) suggesting that AFA_{index} might differ between the three analysed periods. However, no significant differences were found in a post-hoc analysis (Holm-Sidak multiple comparisons test), suggesting that there might be no effect or a very reduced one.

To present another view of how the variance of peaks and troughs over the time window is very small, two graphs were computed showing the time course of average voltage values for peaks and troughs for the two configurations BU and UB (Figure 3.8C and 3.8D). The channels chosen to make this plot were the same ones used in the plots presented in Figure 3.3A and 3.5A.

In both configurations, it can be seen that the peaks and troughs undergo little change over the time window and have the same small changes when comparing each other, that is, when the AFA_{index} formula is computed, when there is practically zero variance either on peaks or troughs, the value of the AFA_{index} will be almost 0. Therefore, these two analyses corroborate the information presented in Figures 3.8A and 3.8B.

3.6. EEG Fluctuations during Stable Periods of Perception

In order to evaluate whether the scalp potential fluctuations measured during periods of perceptual change were a phenomenon lasting longer than the immediate moment preceding or following a perceptual change, we analysed potentials during epochs corresponding to stable periods of perception, encompassing 1 second epochs. Given that the EEG data was intentionally not highpass filtered in a way to remove slow EEG fluctuations (< 0.5 Hz), potentials with very slow kinetics and lasting over 10 secs, i.e. longer than the average duration of a typical individual percept, could be measured along the recording period. Figure 3.9A represents the topography for T-Values calculated for statistical differences between the two configurations Bound and Unbound in epochs of stable perception and referenced by the average. The channels showing statistically significant differences are located in the frontal regions of the left and right hemisphere of the head and also in some occipital and parietal electrodes on the right side. There are negative values in the anterior part of the scalp while positive values are more located in the posterior part. This figure and result is very similar to the one presented in Figure 3.3C, which demonstrates the differences between configurations for a selected time period following the change in perception. There are small differences between the two images, specifically in 3C significant parietal and

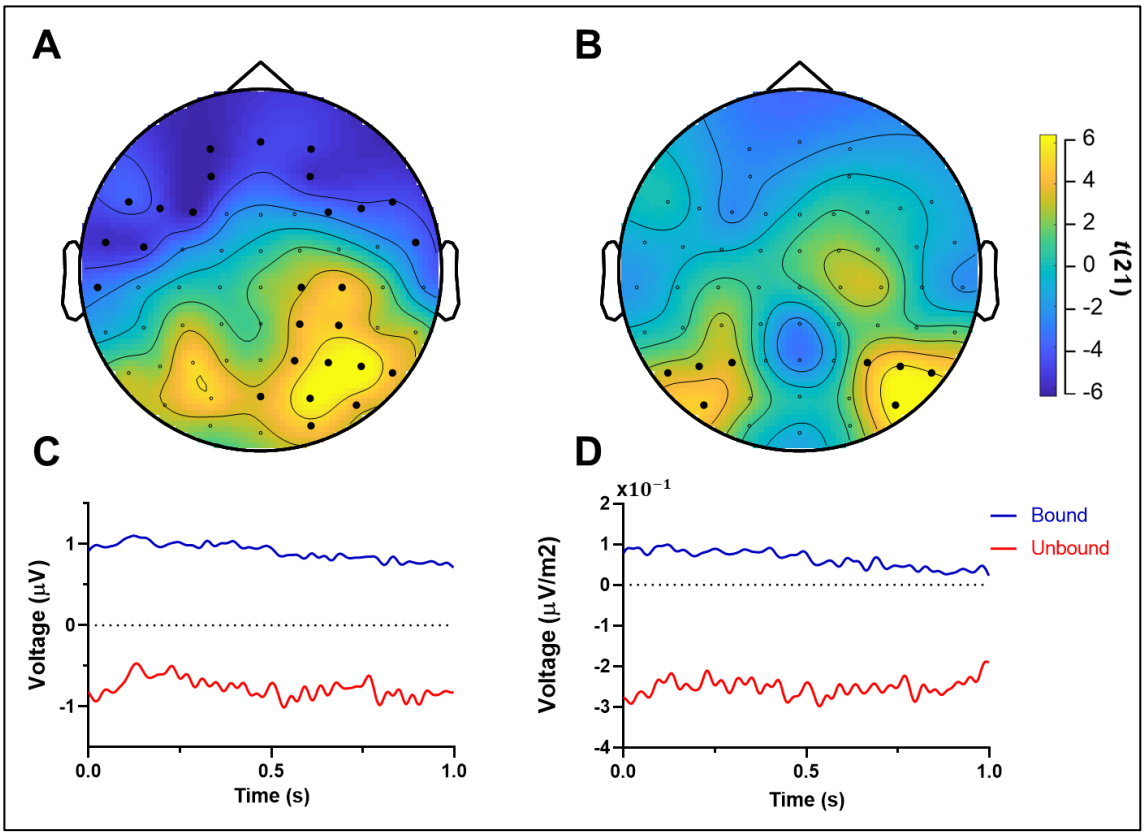

Figure 3.9. Topographies of Differences and Average Time course for Stable Perception Epochs. (**A**) Topographic distribution of T-values achieved with statistical test between epochs with a Stable Perception (SU and SB) with an average reference, with significant channels marked with black dots (cluster-based statistics with Monte Carlo permutations, $p < 0.01$). (**B**) Similar Distribution represented in A but using the reference-free method Surface Laplacian/CSD. Epochs used in both representations last 1 sec. (**C**) Average Time course of potentials of Stable Epochs of channels P2, P4, P6, P8, PO4, PO8, O2 using average reference. (**D**) Similar representation to C but using the reference-free method Surface Laplacian/CSD.

occipital channels are marked on the left side, but from a general point of view the two topographies are quite similar. This reveals that the differences between Bound and Unbound perceptions remain similar even several seconds after the stimulus perceptual change. Differences between perceptions of this ambiguous image had been previously shown to involve beta activity and these were sustained while specific perceptions persisted. Here it appears that these fluctuations in slow potentials are also a phenomenon that spans the duration of a percept.

As for Figure 3.9B, a topography similar to 3.9A is represented, but with the small difference that the data are referenced using the Surface Laplacian/CSD method. Almost the entire scalp is represented by values close to 0, with the exception of the right and left hemispheres at the back of the scalp, which have positive T-Values and statistically significant channels. This topography also has similarities with another that represents a post-change period, Figure 3.5C.

Despite the difference in how the potentials are distributed, this analysis also corroborates the persistence of specific scalp potentials beyond the period of perceptual change.

In Figure 3.9C and 3.9D, a new perspective of the differences between SU and SB conditions is presented. An average of the time course of stable epochs was made in the selected channels throughout this study (P2, P4, P6, P8, PO4 and O2). In Figure 3.9C, an analysis with average reference, it is possible to observe that both conditions remain unchanged and constant throughout the entire duration of the epoch. The SB epochs are perpetuated after the perceptual change with amplitudes of 1 μV and the SU epochs with negative amplitude values of -1 μV. The Unbound condition is the one that still has some variations, but on a small scale, with amplitudes around -0.5 μV. This also happens because this is the least stable perception, hence it is the one that has some variation, albeit without great importance. As for Figure 3.9D, an analysis made with a reference-free method, it is observed that the epochs have a time course similar to those presented in 3.9C with average reference. Both remain stable, with a slight gradual decrease over time for the Bound configuration in the order of 1 μV/m2 of amplitude and small variations for the Unbound configuration, with amplitudes of -1 μV/m2.

These two new representations demonstrate that perceptions are maintained in a constant and relatively invariable way long after the perceptual change in the subjects has been reported and support the information that was presented in Figures 3.9A and 3.9B.

3.7. General Discussion

In summary, the present work aimed to try to understand how beta oscillations are associated with event-related potentials that are evoked during perceptual transitions of ambiguous stimulus. For this, we studied potentials that arise upon perceptual changes during viewing of an ambiguous motion stimulus. These potentials not only are associated with the perceptual change per se but also show differences for distinct percepts. Due to the similar temporal structure of both beta event-related spectral perturbations and the ERPs, a hypothesis that relates asymmetrical oscillations modulation with originating specific components of ERPs was further studied.

As this work progressed, some of the typical shortcomings of studying brain potentials recorded from scalp electrodes led to a further exploration of alternative analysis strategies to better interpret the identified potentials. Starting with the reference problem, this is a long-standing debate among scientists involved in EEG studies. Since the EEG is a relative measure, as each electrode's signal is the difference between the potential in the electrode and the reference electrode, there is currently no consensus choice of the reference that should be used. Consequently, for the analysis not to be biased by the choice of reference, it was decided to carry out two analyses: on a first approach an average reference was selected as it is a common montage that removes significant biases from selecting single channel reference. Upon inspecting the initial results, a second approach was devised using a reference-free method that for the purposes of identifying the sources of the perception related potentials provided greater spatial specificity. Thus, the second analysis with the Surface Laplacian/CSD method demonstrated that it has a greater spatial resolution comparatively with the average reference, as it presents greater specificity of channels with significant differences between the two configurations of perceptual switches.

The regions where these differences are most visible are the parietal and occipital, and are particularly evident in periods that follow the perceptual change, likely due to being a period of greater stability of the upcoming percept. These results make sense in light of the role of the visual cortex in the disambiguation of visual stimuli and

corroborates with studies using functional magnetic resonance imaging (fMRI) that have reciprocal interactions between the MT/V5 region and parietal regions when observing bistable stimuli (Megumi et al., 2015).

The mean ERPs of the channels in the right parieto-occipital region are similar for the two types of reference and demonstrate a positive shift in the switch to Bound perception, while the switch to Unbound perception shows a trend towards negative potentials. This type of reversal is similar to the beta power time course presented in Costa et al. (2017), in which neuroelectric signatures display distinct behaviours and distinguish perceptual outcomes: Unbound perception shows a negative potential and lower beta power values while Bound perception shows a large positive potential and a concurrent increase in beta power.

Similar to the differences in beta activity reported previously that correlate with particular perceptual configurations of ambiguous stimuli, the potentials studied here also appear to extend beyond the time of a perceptual switch. This difference in scalp potentials is mainly observed for occipital areas, hence over the visual cortex, and in the current setting are seen several seconds after a perceptual switch. Typically, ERPs are studied for events that are much shorter, with durations of 100 of milliseconds to 1 or 2 seconds at maximum. The current study employed methods of more accurately measuring these potentials by avoiding high-pass filters and using a reference-free approach. The source and role of these long-lasting potentials is up for debate but appears to match other neurophysiological signals with sustained activity during ambiguous perception. Castelo-Branco and colleagues (2002) had previously shown that hMT shows sustained increased activity when ambiguous perception results in interpreting a figure describing movement along more directions than a single coherent percept (see also Duarte et al. 2017). This phenomenon reveals signals from a constant mode of activity, that can also be observed for gamma activity using more sensitive methods such as MEG and stereoEEG (sEEG; preliminary data). It remains an open question whether these potentials can be seen as a correlate of neuronal states or of modes of activity (feedback vs bottom-up signals) as much as certain frequency bands are seen as playing distinct roles in cortical activity. The regions where these potentials

arise does lend some credence to the hypothesis that extrastriate areas such as hMT are its sources.

Since the ERPs and the power time course of the betas have similar variations for the same types of conditions, it was hypothesized that the slow components observed in the ERPs were directly related to the oscillatory activity of the EEG. This approach was based on the model described in Mazaheri and Jensen, (2008), supporting the idea that the asymmetry of the oscillations could explain the generation of these same components. The AFA_{index} has been shown to be a good indicator for measuring the asymmetry of EEG oscillatory activity. However, it was concluded that the ongoing oscillatory activity does not have asymmetric amplitude and that the peaks and troughs are modulated almost identically. For this reason, the slow components of ERPs cannot be explained by the asymmetry of oscillatory activity.

In the periods in which the perception remains stable, it is concluded that there is no change in the potentials and that these remain for several seconds after the perceptual change. It is also in the stable epochs of Unbound perception that there is greater variation, although it is of little magnitude, but it confirms that this perception is less stable than Bound.

4. Conclusions and Future Work

The work presented in this thesis provided data and information for a better understanding of the relationship between event-related potentials and brain oscillations associated with the perception of ambiguous stimuli. Analysing the dataset obtained from Costa et al. (2017), an ERP analysis and a time frequency analysis were carried out, we proposed to test a hypothesis that associated ERP components with beta asymmetric modulations and also an analysis of the potentials related to periods in which the perception remained stable. Through the results presented in the previous section and the respective discussion, we conclude that the Surface Laplacian/CSD reference method is a good choice for EEG studies that require a good spatial resolution and that there is a relationship between the activation of beta waves and the observed slow components in ERPs. The modulation of both happens in a similar way over the time window of periods in which a change of perception occurs, but, however, this relationship cannot be explained by the asymmetry of the amplitude of the oscillatory activity in this frequency range (13-30 Hz). We also concluded that the potentials captured in the regions selected in the study remain constant and with little variation when the visual perception of the stimulus remains stable. So, it remains open what role beta oscillations play in evoked potentials for a perceptual change.

In a future work, this issue could be better explored through a source analysis to better understand the mechanisms and regions that are associated with the observed potentials or verify for the same experiment and with the same conditions, the fields generated but with data acquisition through of MEG. MEG data is naturally reference free and has greater scalp coverage and higher spatial resolution. In this way, it would be possible to assess whether the phenomenon recorded in the EEG data manifests itself in the same way as described in this work. It should be noted that the MEG data for this experiment exist and have already been acquired.

5. Bibliography

Anzai, A., Peng, X. and Van Essen, D.C. (2007). Neurons in monkey visual area V2 encode combinations of orientations. Nature Neuroscience, 10(10), pp.1313–1321. doi: https://doi.org/10.1038/nn1975.

Başar-Eroglu, C., Strüber, D., Kruse, P., Başar, E. and Stadler, M. (1996). Frontal gamma-band enhancement during multistable visual perception. International Journal of Psychophysiology, 24(1-2), pp.113–125. doi: https://doi.org/10.1016/s0167-8760(96)00055-4.

Başar-Eroglu, C., Strüber, D., Stadler, M., Kruse, P. and Başar, E. (1993). Multistable Visual Perception Induces a Slow Positive EEG Wave. International Journal of Neuroscience, 73(1- 2), pp.139–151. doi: https://doi.org/10.3109/00207459308987220.

Bastiaansen, M., Mazaheri, A. and Jensen, O. (2011). Beyond ERPs: Oxford Handbooks Online. Oxford University Press. doi: https://doi.org/10.1093/oxfordhb/9780195374148.013.0024.

Bentin, S., Allison, T., Puce, A., Perez, E. and McCarthy, G. (1996). Electrophysiological Studies of Face Perception in Humans. Journal of Cognitive Neuroscience, 8(6), pp.551–565. doi: https://doi.org/10.1162/jocn.1996.8.6.551.

Berger, H. (1929). Über das Elektrenkephalogramm des Menschen. Archiv für Psychiatrie und Nervenkrankheiten, 87(1), pp.527–570. doi: https://doi.org/10.1007/bf01797193.

Brainard, D.H. (1997). The Psychophysics Toolbox. Spatial Vision, 10(4), pp.433–436. doi: https://doi.org/10.1163/156856897x00357.

Brascamp, J.W. and Shevell, S.K. (2021). The Certainty of Ambiguity in Visual Neural Representations. Annual Review of Vision Science, 7(1), pp.465–486. doi: https://doi.org/10.1146/annurev-vision-100419-125929.

Buzsaki, G. (2004). Neuronal Oscillations in Cortical Networks. Science, 304(5679), pp.1926–1929. doi: https://doi.org/10.1126/science.1099745.

Buzsáki, G. and Wang, X.-J. (2012). Mechanisms of Gamma Oscillations. Annual Review of Neuroscience, 35(1), pp.203–225. doi: https://doi.org/10.1146/annurev-neuro-062111-150444.

Buzsáki, G., Anastassiou, C.A. and Koch, C. (2012). The origin of extracellular fields and currents — EEG, ECoG, LFP and spikes. Nature Reviews Neuroscience, 13(6), pp.407–420. doi: https://doi.org/10.1038/nrn3241.

Castelo-Branco, M., Formisano, E., Backes, W., Zanella, F., Neuenschwander, S., Singer, W. and Goebel, R. (2002). Activity patterns in human motion-sensitive areas depend on the interpretation of global motion. Proceedings of the National Academy of Sciences, 99(21), pp.13914–13919. doi: https://doi.org/10.1073/pnas.202049999.

Castelo-Branco, M., Goebel, R., Neuenschwander, S. and Singer, W. (2000). Neural synchrony correlates with surface segregation rules. Nature, 405(6787), pp.685–689. doi: https://doi.org/10.1038/35015079.

Cavanaugh, J., Berman, R.A., Joiner, W.M. and Wurtz, R.H. (2016). Saccadic Corollary Discharge Underlies Stable Visual Perception. Journal of Neuroscience, 36(1), pp.31–42. doi: https://doi.org/10.1523/jneurosci.2054-15.2016.

Chatrian, G.E., Lettich, E. and Nelson, P.L. (1985). Ten Percent Electrode System for Topographic Studies of Spontaneous and Evoked EEG Activities. American Journal of EEG Technology, 25(2), pp.83–92. doi: https://doi.org/10.1080/00029238.1985.11080163.

Cohen, M.X. (2014). Analyzing neural time series data: theory and practice. Cambridge, Massachusetts: The Mit Press.

Cooper, R., Winter, A.L., Crow, H.J. and Walter, W.Grey. (1965). Comparison of subcortical, cortical and scalp activity using chronically indwelling electrodes in man. Electroencephalography and Clinical Neurophysiology, 18(3), pp.217–228. doi: https://doi.org/10.1016/0013-4694(65)90088-x.

Costa, G.N., Duarte, J.V., Martins, R., Wibral, M. and Castelo-Branco, M. (2017). Interhemispheric Binding of Ambiguous Visual Motion Is Associated with Changes in Beta Oscillatory Activity but Not with Gamma Range Synchrony. Journal of Cognitive Neuroscience, 29(11), pp.1829–1844. doi: https://doi.org/10.1162/jocn_a_01158.

Csicsvari, J., Jamieson, B., Wise, K.D. and Buzsáki, G. (2003). Mechanisms of Gamma Oscillations in the Hippocampus of the Behaving Rat. Neuron, 37(2), pp.311–322. doi: https://doi.org/10.1016/s0896-6273(02)01169-8

Delorme, A. and Makeig, S. (2004). EEGLAB: an open source toolbox for analysis of single-trial EEG dynamics including independent component analysis. Journal of Neuroscience Methods, 134(1), pp.9–21. doi: https://doi.org/10.1016/j.jneumeth.2003.10.009.

Engel, A.K. and Fries, P. (2010). Beta-band oscillations—signalling the status quo? Current Opinion in Neurobiology, 20(2), pp.156–165. doi: https://doi.org/10.1016/j.conb.2010.02.015.

Engel, A.K., Fries, P. and Singer, W. (2001). Dynamic predictions: Oscillations and synchrony in top–down processing. Nature Reviews Neuroscience, 2(10), pp.704–716. doi: https://doi.org/10.1038/35094565.

Epstein, C.M. (2003). Aliasing in the visual EEG: a potential pitfall of video display technology. Clinical Neurophysiology, 114(10), pp.1974–1976. doi: https://doi.org/10.1016/s1388-2457(03)00168-8.

Gloor, P. (1969). Hans Berger on Electroencephalography. American Journal of EEG Technology, 9(1), pp.1–8. doi: https://doi.org/10.1080/00029238.1969.11080728.

Goodale, M.A. (2011). Transforming vision into action. Vision Research, 51(13), pp.1567–1587. doi: https://doi.org/10.1016/j.visres.2010.07.027.

Gregory, R.L. (1997). Knowledge in perception and illusion. Philosophical Transactions of the Royal Society of London. Series B: Biological Sciences, 352(1358), pp.1121–1127. doi: https://doi.org/10.1098/rstb.1997.0095.

Hanslmayr, S., Klimesch, W., Sauseng, P., Gruber, W., Doppelmayr, M., Freunberger, R., Pecherstorfer, T. and Birbaumer, N. (2006). Alpha Phase Reset Contributes to the Generation of ERPs. Cerebral Cortex, 17(1), pp.1–8. doi: https://doi.org/10.1093/cercor/bhj129.

Heitmann, S., Gong, P. and Breakspear, M. (2012). A computational role for bistability and traveling waves in motor cortex. Frontiers in Computational Neuroscience, 6. doi: https://doi.org/10.3389/fncom.2012.00067.

Helfrich, R.F., Becker, H.G.T. and Haarmeier, T. (2012). Processing of Coherent Visual Motion in Topographically Organized Visual Areas in Human Cerebral Cortex. Brain Topography, 26(2), pp.247–263. doi: https://doi.org/10.1007/s10548-012-0226-1.

Huff, T. and Prasanna Tadi (2019). Neuroanatomy, Visual Cortex. Nih.gov. Available at: https://www.ncbi.nlm.nih.gov/books/NBK482504/.

İşoğlu-Alkaç, Ü. and Strüber, D. (2006). Necker cube reversals during long-term EEG recordings: Sub-bands of alpha activity. International Journal of Psychophysiology, 59(2), pp.179–189. doi: https://doi.org/10.1016/j.ijpsycho.2005.05.002.

Jasper, H.H. (1958). The ten±twenty electrode system of the International Federation. Electroencephalography and Clinical Neurophysiology, 10, pp. 371-375.

Junghöfer, M., Elbert, T., Tucker, D.M. and Braun, C. (1999). The polar average reference effect: a bias in estimating the head surface integral in EEG recording. Clinical Neurophysiology, 110(6), pp.1149–1155. doi: https://doi.org/10.1016/s1388-2457(99)00044-9.

Kaas, J.H. and Collins, C.E. eds., (2003). The Primate Visual System. doi: https://doi.org/10.1201/9780203507599.

Katyal, S., He, S., He, B. and Engel, S.A. (2019). Frequency of alpha oscillation predicts individual differences in perceptual stability during binocular rivalry. Human Brain Mapping, 40(8), pp.2422–2433. doi: https://doi.org/10.1002/hbm.24533.

Kayser, J. and Tenke, C.E. (2015). Issues and considerations for using the scalp surface Laplacian in EEG/ERP research: A tutorial review. International Journal of Psychophysiology, 97(3), pp.189–209. doi: https://doi.org/10.1016/j.ijpsycho.2015.04.012.

Kayser, J. and Tenke, C.E. (2015). On the benefits of using surface Laplacian (Current Source Density) methodology in electrophysiology. International journal of psychophysiology: official journal of the International Organization of Psychophysiology, 97(3), pp.171–173. doi: https://doi.org/10.1016/j.ijpsycho.2015.06.001.

Kilner, J.M., Vargas, C., Duval, S., Blakemore, S.-J. and Sirigu, A. (2004). Motor activation prior to observation of a predicted movement. Nature Neuroscience, 7(12), pp.1299–1301. doi: https://doi.org/10.1038/nn1355.

Kopell, N., Ermentrout, G.B., Whittington, M.A. and Traub, R.D. (2000). Gamma rhythms and beta rhythms have different synchronization properties. Proceedings of the National Academy of Sciences, 97(4), pp.1867–1872. doi: https://doi.org/10.1073/pnas.97.4.1867.

Kornmeier, J. and Bach, M. (2012). Ambiguous Figures – What Happens in the Brain When Perception Changes But Not the Stimulus. Frontiers in Human Neuroscience, 6. doi: https://doi.org/10.3389/fnhum.2012.00051.

Kutas, M. e Hillyard, S. (1980) 'Reading senseless sentences: brain potentials reflect semantic incongruity', Science, 207(4427), pp. 203–205. doi: https://doi.org/10.1126/science.7350657.

Lei, X. and Liao, K. (2017). Understanding the Influences of EEG Reference: A Large-Scale Brain Network Perspective. Frontiers in Neuroscience, 11. doi: https://doi.org/10.3389/fnins.2017.00205.

Lorenceau, J., Shiffrar, M., Wells, N. and Castet, E. (1993). Different motion sensitive units are involved in recovering the direction of moving lines. Vision Research, 33(9), pp.1207–1217. doi: https://doi.org/10.1016/0042-6989(93)90209-f.

Luck, S.J. (2014). An introduction to the event-related potential technique. Cambridge, Mass.: Mit Press.

Luck, S.J. and Kappenman, E.S. (2011). ERP Components and Selective Attention. Oxford Handbooks Online. Oxford University Press. doi: https://doi.org/10.1093/oxfordhb/9780195374148.013.0144.

Makeig, S., Westerfield, M., Jung, T. P., Enghoff, S., Townsend, J., Courchesne, E., & Sejnowski, T. J. (2002). Dynamic brain sources of visual evoked responses. Science, 295(5555), pp.690–694. doi: https://doi.org/10.1126/science.1066168.

Mäkinen, V., Tiitinen, H. and May, P. (2005). Auditory event-related responses are generated independently of ongoing brain activity. NeuroImage, 24(4), pp.961–968. doi: https://doi.org/10.1016/j.neuroimage.2004.10.020.

Maris, E. and Oostenveld, R. (2007). Nonparametric statistical testing of EEG- and MEG-data. Journal of Neuroscience Methods, 164(1), pp.177–190. doi: https://doi.org/10.1016/j.jneumeth.2007.03.024.

Marturano, F., Brigadoi, S., Doro, M., Dell'Acqua, R. and Sparacino, G. (2020). A Time-Frequency Analysis for the Online Detection of the N2pc Event-Related Potential (ERP) Component in Individual EEG Datasets. 2020 42nd Annual International Conference of the IEEE Engineering in Medicine & Biology Society (EMBC). doi: https://doi.org/10.1109/embc44109.2020.9175462.

Masson, G.S. and Ilg, U.J. (2010). Dynamics of Visual Motion Processing: Neuronal, Behavioral, and Computational Approaches. New York, Ny: Springer Us.

Mather, G. (2010). Motion perception: behavior and neural substrate. Wiley Interdisciplinary Reviews: Cognitive Science, 2(3), pp.305–314. doi: https://doi.org/10.1002/wcs.110.

Mather, G. (2016). Foundations of Sensation and Perception. Psychology Press. doi: https://doi.org/10.4324/9781315672236.

Mathes, B., Strüber, D., Stadler, M.A. and Basar-Eroglu, C. (2006). Voluntary control of Necker cube reversals modulates the EEG delta- and gamma-band response. Neuroscience Letters, 402(1-2), pp.145–149. doi: https://doi.org/10.1016/j.neulet.2006.03.063.

Mazaheri, A. and Jensen, O. (2008). Asymmetric Amplitude Modulations of Brain Oscillations Generate Slow Evoked Responses. Journal of Neuroscience, 28(31), pp.7781– 7787. doi: https://doi.org/10.1523/jneurosci.1631-08.2008.

Megumi, F., Bahrami, B., Kanai, R. and Rees, G. (2015). Brain activity dynamics in human parietal regions during spontaneous switches in bistable perception. NeuroImage, 107, pp.190–197. doi: https://doi.org/10.1016/j.neuroimage.2014.12.018.

Movshon, J, Adelson, EH, Gizzi, MS & Newsome, WT 1985, The analysis of moving visual patterns. in C Chagas, R Gattass & C Gross (eds), Pattern recognition mechanisms. Pontificiae Academiae Scientiarum Scripta Varia, vol. 54, Vatican Press, Rome, pp. 117-151.

Müller-Putz, G.R. (2020). Electroencephalography. Brain-Computer Interfaces, pp.249–262. doi: https://doi.org/10.1016/b978-0-444-63934-9.00018-4.

Näätänen, R., Gaillard, A.W.K. and Mäntysalo, S. (1978). Early selective-attention effect on evoked potential reinterpreted. Acta Psychologica, 42(4), pp.313–329. doi: https://doi.org/10.1016/0001-6918(78)90006-9.

Nakhla, N., Korkian, Y., Krause, M.R. and Pack, C.C. (2020). Neural Selectivity for Visual Motion in Macaque Area V3A. eneuro, 8(1), pp.ENEURO.0383-20.2020. doi: https://doi.org/10.1523/eneuro.0383-20.2020.

Nikulin, V.V., Linkenkaer-Hansen, K., Nolte, G., Lemm, S., Müller, K.R., Ilmoniemi, R.J. and Curio, G. (2007). A novel mechanism for evoked responses in the human brain. European Journal of Neuroscience, 25(10), pp.3146–3154. doi: https://doi.org/10.1111/j.1460-9568.2007.05553.x.

Nunez, P.L. and Ramesh Srinivasan (2006). Electric fields of the brain: the neurophysics of EEG. Oxford: Oxford University Press.

Okazaki, M., Kaneko, Y., Yumoto, M. and Arima, K. (2008). Perceptual change in response to a bistable picture increases neuromagnetic beta-band activities. Neuroscience Research, 61(3), pp.319–328. doi: https://doi.org/10.1016/j.neures.2008.03.010.

Oostenveld, R. and Praamstra, P. (2001). The five percent electrode system for high-resolution EEG and ERP measurements. Clinical Neurophysiology, 112(4), pp.713–719. doi: https://doi.org/10.1016/s1388-2457(00)00527-7.

Oostenveld, R., Fries, P., Maris, E. and Schoffelen, J.-M. (2011). FieldTrip: Open Source Software for Advanced Analysis of MEG, EEG, and Invasive Electrophysiological Data. Computational Intelligence and Neuroscience, 2011, pp.1–9. doi: https://doi.org/10.1155/2011/156869.

Pack, C.C. and Born, R.T. (2008). Cortical Mechanisms for the Integration of Visual Motion. The Senses: A Comprehensive Reference, pp.189–218. doi: https://doi.org/10.1016/b978-012370880-9.00309-1.

Pack, C.C., Livingstone, M.S., Duffy, K.R. and Born, R.T. (2003). End-Stopping and the Aperture Problem. Neuron, 39(4), pp.671–680. doi: https://doi.org/10.1016/s0896-6273(03)00439-2.

Perrin, F., Pernier, J., Bertrand, O. and Echallier, J.F. (1989). Spherical splines for scalp potential and current density mapping. Electroencephalography and Clinical Neurophysiology, 72(2), pp.184–187. doi: https://doi.org/10.1016/0013-4694(89)90180-6.

Piantoni, G., Kline, K.A. and Eagleman, D.M. (2010). Beta oscillations correlate with the probability of perceiving rivalrous visual stimuli. Journal of Vision, 10(13), pp.18–18. doi: https://doi.org/10.1167/10.13.18.

Piantoni, G., Romeijn, N., Gomez-Herrero, G., Van Der Werf, Y.D. and Van Someren, E.J.W. (2017). Alpha Power Predicts Persistence of Bistable Perception. Scientific Reports, 7(1). doi: https://doi.org/10.1038/s41598-017-05610-8.

Pitzalis, S., Fattori, P. and Galletti, C. (2015). The human cortical areas V6 and V6A. Visual Neuroscience, 32. doi: https://doi.org/10.1017/s0952523815000048.

Pitzalis, S., Serra, C., Sulpizio, V., Committeri, G., Pasquale, F., Fattori, P., Galletti, C., Sepe, R. and Galati, G. (2019). Neural bases of self- and object-motion in a naturalistic vision. Human Brain Mapping, 41(4), pp.1084–1111. doi: https://doi.org/10.1002/hbm.24862.

Purves, D. (2018). Neuroscience. New York: Oxford University Press.

Rabin, J., Houser, B., Talbert, C. and Patel, R. (2016). Blue-Black or White-Gold? Early Stage Processing and the Color of 'The Dress'. PLoS ONE, 11(8). doi: https://doi.org/10.1371/journal.pone.0161090.

Rangaswamy, M., Jones, K.A., Porjesz, B., Chorlian, D.B., Padmanabhapillai, A., Kamarajan, C., Kuperman, S., Rohrbaugh, J., O'Connor, S.J., Bauer, L.O., Schuckit, M.A. and Begleiter, H. (2007). Delta and theta oscillations as risk markers in adolescent offspring of alcoholics. International Journal of Psychophysiology, 63(1), pp.3–15. doi: https://doi.org/10.1016/j.ijpsycho.2006.10.003.

Regan, D. (1989). Human Brain Electrophysiology. New York: Elsevier.

Rider, A.T., Nishida, S. and Johnston, A. (2016). Multiple-stage ambiguity in motion perception reveals global computation of local motion directions. Journal of Vision, 16(15), p.7. doi: https://doi.org/10.1167/16.15.7.

Salisbury, D.F., Rutherford, B., Shenton, M.E. and McCarley, R.W. (2001). Button-pressing affects P300 amplitude and scalp topography. Clinical Neurophysiology, 112(9), pp.1676–1684. doi: https://doi.org/10.1016/s1388-2457(01)00607-1.

Sauseng, P., Klimesch, W., Gruber, W.R., Hanslmayr, S., Freunberger, R. and Doppelmayr, M. (2007). Are event-related potential components generated by phase resetting of brain oscillations? A critical discussion. Neuroscience, 146(4), pp.1435–1444. doi: https://doi.org/10.1016/j.neuroscience.2007.03.014.

Schomer, D.L. and Lopes, F. (2012). Niedermeyer's Electroencephalography. Lippincott Williams & Wilkins.

Schwartz, J.-L., Grimault, N., Hupé, J.-M., Moore, B.C.J. and Pressnitzer, D. (2012). Multistability in perception: binding sensory modalities, an overview. Philosophical Transactions of the Royal Society B: Biological Sciences, 367(1591), pp.896–905. doi: https://doi.org/10.1098/rstb.2011.0254.

Shah, A. S., Bressler, S. L., Knuth, K. H., Ding, M., Mehta, A. D., Ulbert, I., & Schroeder, C. E. (2004). Neural dynamics and the fundamental mechanisms of event-related brain potentials. Cerebral cortex, 14(5), pp.476–483. doi: https://doi.org/10.1093/cercor/bhh009.

Srinivasan, R., Winter, W.R., Ding, J. and Nunez, P.L. (2007). EEG and MEG coherence: Measures of functional connectivity at distinct spatial scales of neocortical dynamics. Journal of Neuroscience Methods, 166(1), pp.41–52. doi: https://doi.org/10.1016/j.jneumeth.2007.06.026.

Stone, J.V. (2002). Independent component analysis: an introduction. Trends in Cognitive Sciences, 6(2), pp.59–64. doi: https://doi.org/10.1016/s1364-6613(00)01813-1.

Strüber, D. and Herrmann, C.S. (2002). MEG alpha activity decrease reflects destabilization of multistable percepts. Cognitive Brain Research, 14(3), pp.370–382. doi: https://doi.org/10.1016/s0926-6410(02)00139-8.

Strüber, D., Başar-Eroglu, C., Miener, M. and Stadler, M. (2001). EEG gamma-band response during the perception of Necker cube reversals. Visual Cognition, 8(3-5), pp.609–621. doi: https://doi.org/10.1080/13506280143000151.

Sutton, S., Braren, M., Zubin, J. and John, E.R. (1965). Evoked-potential correlates of stimulus uncertainty. Science (New York, N.Y.), 150(3700), pp.1187–8. doi: https://doi.org/10.1126/science.150.3700.1187.

Tamura, K., Karube, C., Mizuba, T. and Iramina, K. (2012). ERP and time frequency analysis of response to subject's own name. The 5th 2012 Biomedical Engineering International Conference. doi: https://doi.org/10.1109/bmeicon.2012.6465434.

Teichmann, L., Edwards, G. and Baker, C.I. (2021). Resolving visual motion through perceptual gaps. Trends in Cognitive Sciences, 25(11), pp.978–991. doi: https://doi.org/10.1016/j.tics.2021.07.017.

Tong, F. (2003). Primary visual cortex and visual awareness. Nature Reviews Neuroscience, 4(3), pp.219–229. doi: https://doi.org/10.1038/nrn1055.

Tsuchiya, N., Wilke, M., Frässle, S. and Lamme, V.A.F. (2015). No-Report Paradigms: Extracting the True Neural Correlates of Consciousness. Trends in Cognitive Sciences, 19(12), pp.757–770. doi: https://doi.org/10.1016/j.tics.2015.10.002.

VanRullen, R. (2006). The Continuous Wagon Wheel Illusion Is Associated with Changes in Electroencephalogram Power at 13 Hz. Journal of Neuroscience, 26(2), pp.502–507.doi: https://doi.org/10.1523/jneurosci.4654-05.2006.

Vogel, E.K., McCollough, A.W. and Machizawa, M.G. (2005). Neural measures reveal individual differences in controlling access to working memory. Nature, 438(7067), pp.500–503. doi: https://doi.org/10.1038/nature04171.

Wallach, H. (1935). Über visuell wahrgenommene Bewegungsrichtung. Psychologische Forschung, 20(1), pp.325–380. doi: https://doi.org/10.1007/bf02409790.

Walter, W.G., Cooper, R., Aldrige, V.J., McCallum, W.C. and Winter, A.L. (1964). Contingent Negative Variation: An Electric Sign of Sensori-Motor Association and Expectancy in the Human Brain. Nature, 203(4943), pp.380–384. doi: https://doi.org/10.1038/203380a0.

Wandell, B.A., Dumoulin, S.O. and Brewer, A.A. (2007). Visual Field Maps in Human Cortex. Neuron, 56(2), pp.366–383. doi: https://doi.org/10.1016/j.neuron.2007.10.012.

Wang, L., Jensen, O., van den Brink, D., Weder, N., Schoffelen, J.-M., Magyari, L., Hagoort, P. and Bastiaansen, M. (2012). Beta oscillations relate to the N400m during language comprehension. Human Brain Mapping, 33(12), pp.2898–2912. doi: https://doi.org/10.1002/hbm.21410.

Wuerger, S., Shapley, R. and Rubin, N. (1996). 'On the Visually Perceived Direction of Motion' by Hans Wallach: 60 Years Later. Perception, 25(11), pp.1317–1367. doi: https://doi.org/10.1068/p251317.

Yao, D. (2017). Is the Surface Potential Integral of a Dipole in a Volume Conductor Always Zero? A Cloud Over the Average Reference of EEG and ERP. Brain Topography, 30(2), pp.161–171. doi: https://doi.org/10.1007/s10548-016-0543-x.

Yao, D., Qin, Y., Hu, S., Dong, L., Bringas Vega, M.L. and Valdés Sosa, P.A. (2019). Which Reference Should We Use for EEG and ERP practice? Brain Topography, 32(4), pp.530–549. doi: https://doi.org/10.1007/s10548-019-00707-x.

Yordanova, J., Falkenstein, M., Hohnsbein, J. and Kolev, V. (2004). Parallel systems of error processing in the brain. NeuroImage, 22(2), pp.590–602. doi: https://doi.org/10.1016/j.neuroimage.2004.01.040.

Zaretskaya, N. and Bartels, A. (2015). Gestalt perception is associated with reduced parietal beta oscillations. NeuroImage, 112, pp.61–69. doi: https://doi.org/10.1016/j.neuroimage.2015.02.049.

Zeki, S. (2015). Area V5—a microcosm of the visual brain. Frontiers in Integrative Neuroscience, 9. doi: https://doi.org/10.3389/fnint.2015.00021.

Zhu, M., Hardstone, R. and He, B.J. (2022). Neural oscillations promoting perceptual stability and perceptual memory during bistable perception. Scientific Reports, 12(1). doi: https://doi.org/10.1038/s41598-022-06570-4.